

Modern Astronomy

Part 1. Interstellar Medium (ISM)

Lecture 4

March 24 (Monday), 2025

updated 02/24, 15:00

선광일 (Kwang-Il Seon)

UST / KASI

Dust

Dust matters!

- Importance of Dust
 - In our Galaxy, **the gas-to-dust ratio is about 100:1 by mass.** Since the ISM is about 10% of the baryonic mass of the Galaxy, dust grains comprise roughly 0.1% of the total baryonic mass.
 - Dust grains absorb roughly 30-50% of the starlight emitted by the Galaxy and re-emit it as far-infrared continuum emission. ***This means that only 0.1% of the baryons are ultimately responsible for a third to a half of the bolometric luminosity of the Galaxy.***
 - Dust grains are central to the chemistry of interstellar gas. ***The abundance of H₂ in the ISM can only be understood if catalysis on dust grains is the dominant formation avenue.***
 - The formation of planetary systems is believed to begin when dust grains in a protostellar disk begin to coagulate into larger grains, leading to planetesimals and eventually to planets, carrying their complex organic molecules with them.

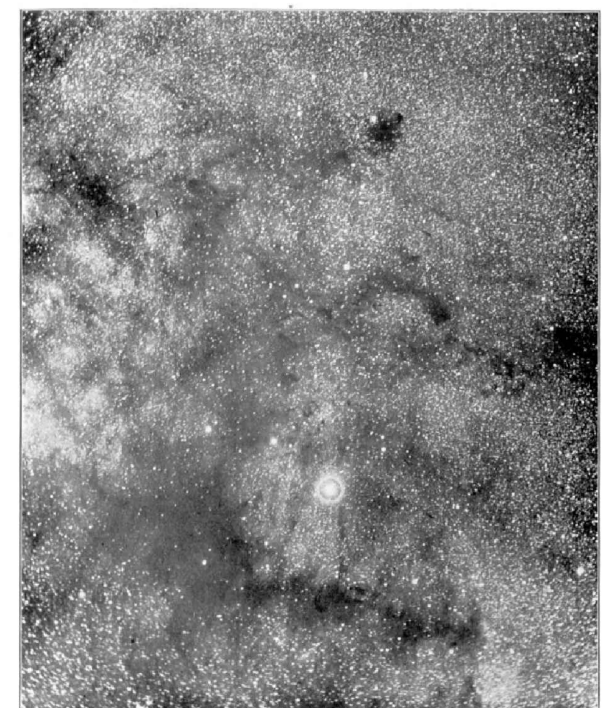
Observed Properties

- **Extinction = Absorption + Scattering**
 - Dust particles can scatter light, changing its direction of propagation. When we look at a reflection nebula, like that surrounding the Pleiades, we are seeing light from the central stars that has been scattered by dust into our line of sight.
 - Dust particles can also absorb light. The relative amount of scattering and absorbing depends on the properties of the dust grains.
- **Thermal radiation from Dust**
 - When dust absorbs light, it becomes warmer, so dust grains can emit light in the form of thermal radiation. Most of this emission is at wavelengths from a few microns (near IR) to the sub-mm range (Far-IR).
- **Polarization**
 - The polarization of starlight was discovered in 1949 (Hall 1949).
 - The degree of polarization tends to be larger for stars with greater reddening, and stars in a given region of the sky tends to have similar polarization directions.



The Pleiades cluster and surrounding reflection nebulae (Fig. 6.3, Ryden)

PLATE II.



PHOTOGRAPH OF THE MILKY WAY NEAR THE STAR THETA OPHIUCHI.

The dark structures near θ Ophiuchi
(Barnard 1899; Fig. 6.1, Ryden)

Extinction

- ***Extinction***

- Astronomers characterize the attenuating effects of dust by the “extinction” A_λ at wavelength λ . The extinction at a particular wavelength λ , measured in “magnitudes” is defined by the difference between the observed magnitude m_λ and the unabsorbed magnitude m_λ^0 :

$$\begin{aligned} A_\lambda \text{ [mag]} &= m_\lambda - m_\lambda^0 \\ &= -2.5 \log_{10} \left(\frac{F_\lambda}{F_\lambda^0} \right) \end{aligned}$$

F_λ = the observed flux from the star

F_λ^0 = the flux that would have been observed if the only attenuation had been from the inverse square law.

- The extinction measured in magnitudes is proportional to the optical depth:

$$F_\lambda = F_\lambda^0 e^{-\tau_\lambda}$$

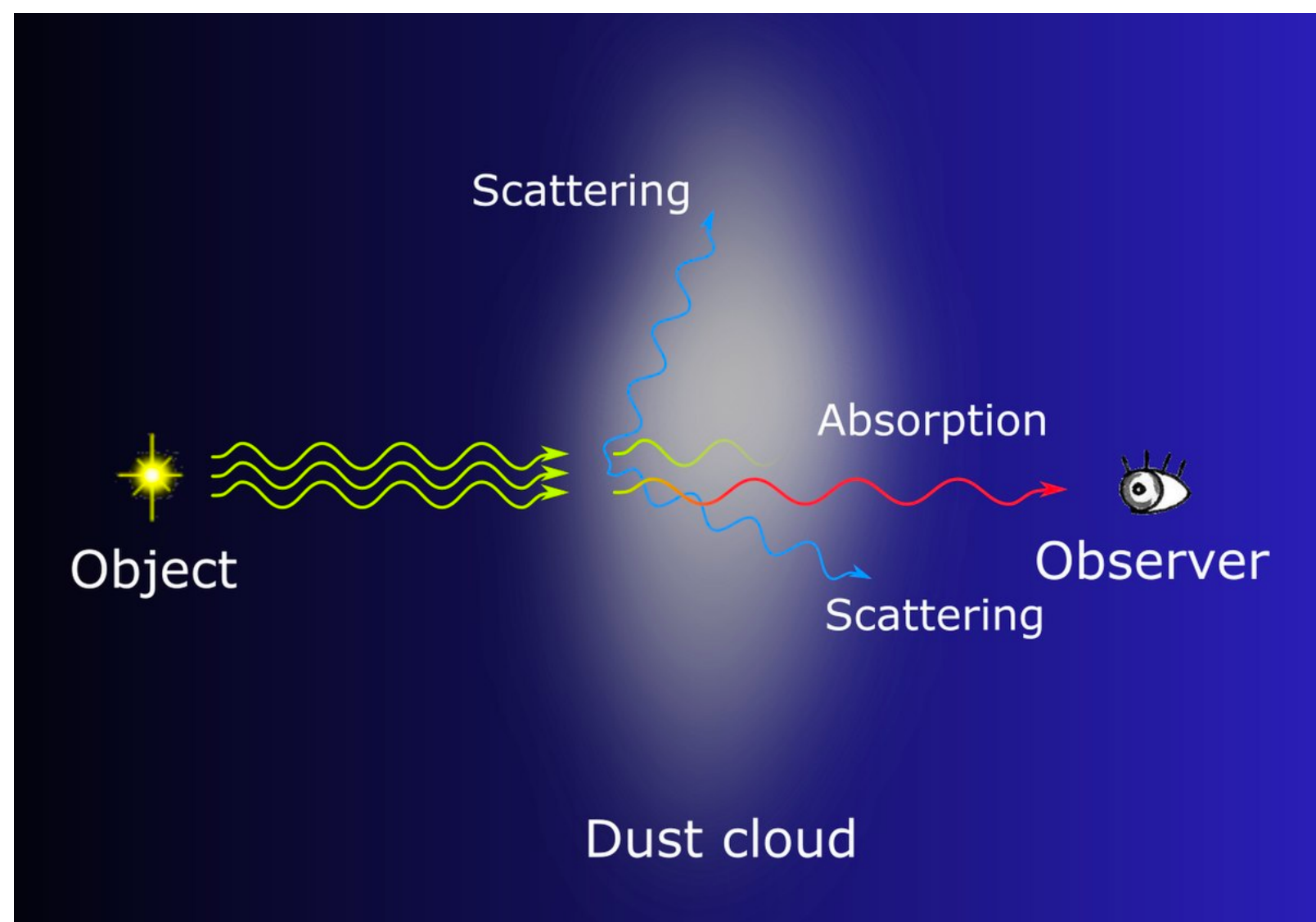


$$\begin{aligned} A_\lambda &= 2.5 \log_{10} (e^{\tau_\lambda}) = 2.5 \log (e) \times \tau_\lambda \\ &= 1.086 \tau_\lambda \end{aligned}$$

Reddening

- ***Reddening***

- Reddening is the phenomena of the color of a visible astronomical object (e.g., star) appearing more red from a distance than from nearby.
- Within the visible wavelength range, **the absorption/scattering cross-section by dust increases with frequency, absorbing/scattering more of the blue light than red.**
- This effect leads to the reddening.



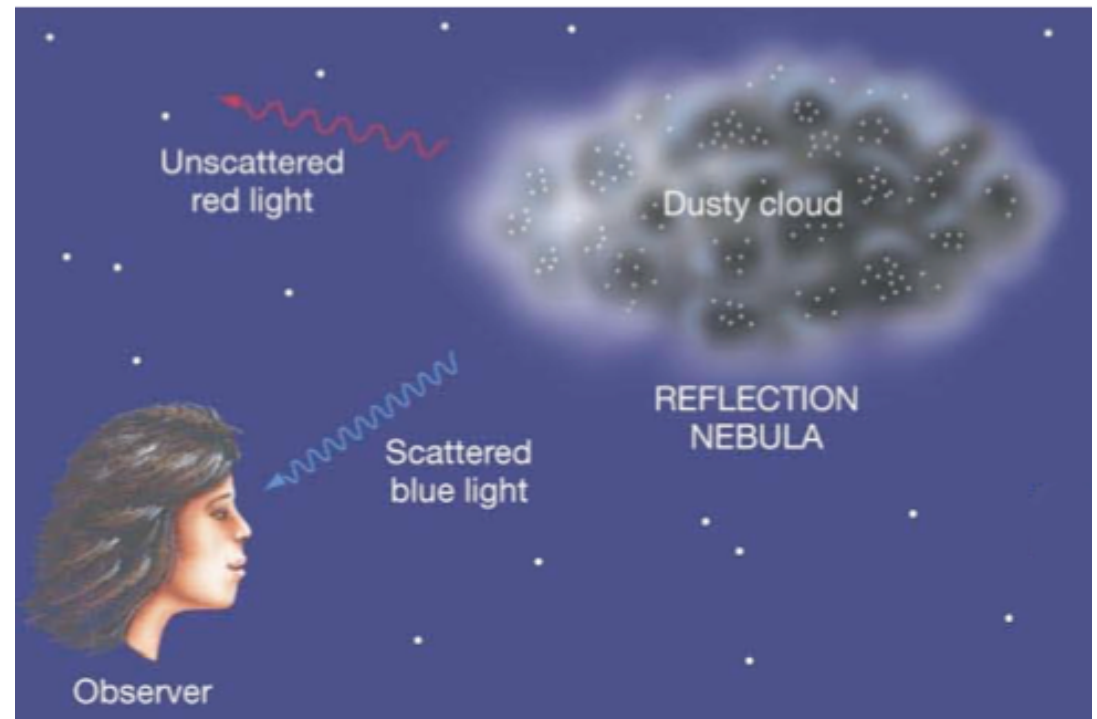
Blue Reflection Nebulae

- ***Scattering of Starlight***

- When an interstellar cloud happens to be unusually near one or more bright stars, we have a reflection nebula, where we see starlight photons that have been scattered by the dust in the cloud.

- ***The spectrum of the light coming from the cloud surface shows the stellar absorption lines***, thus demonstrating that scattering rather than some emission process is responsible.

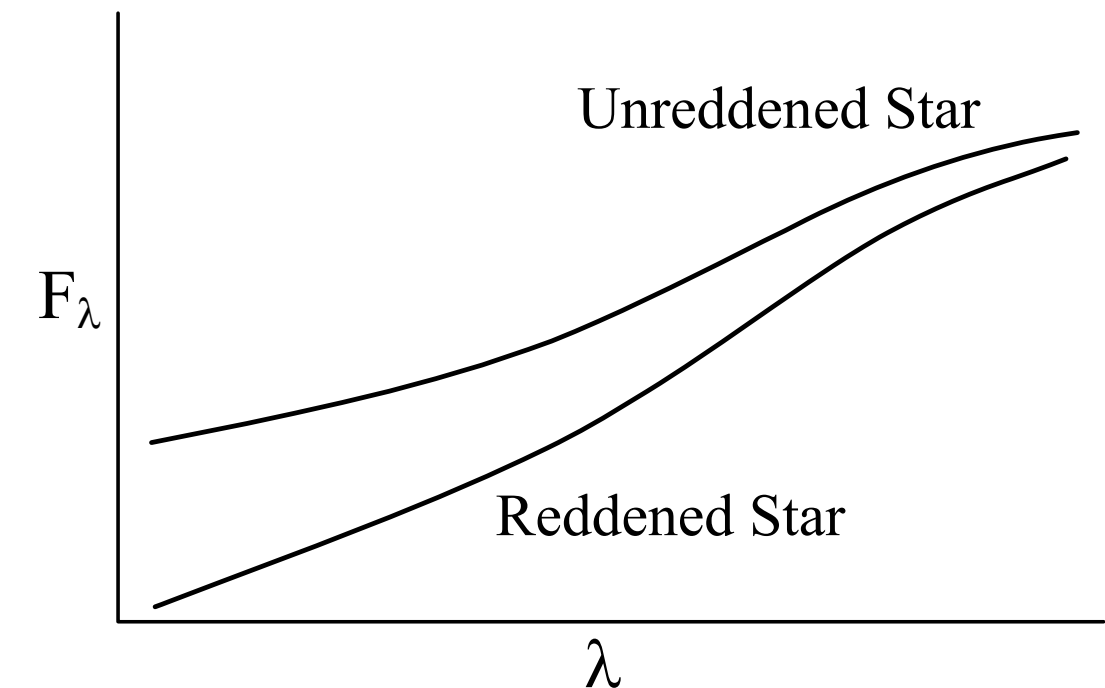
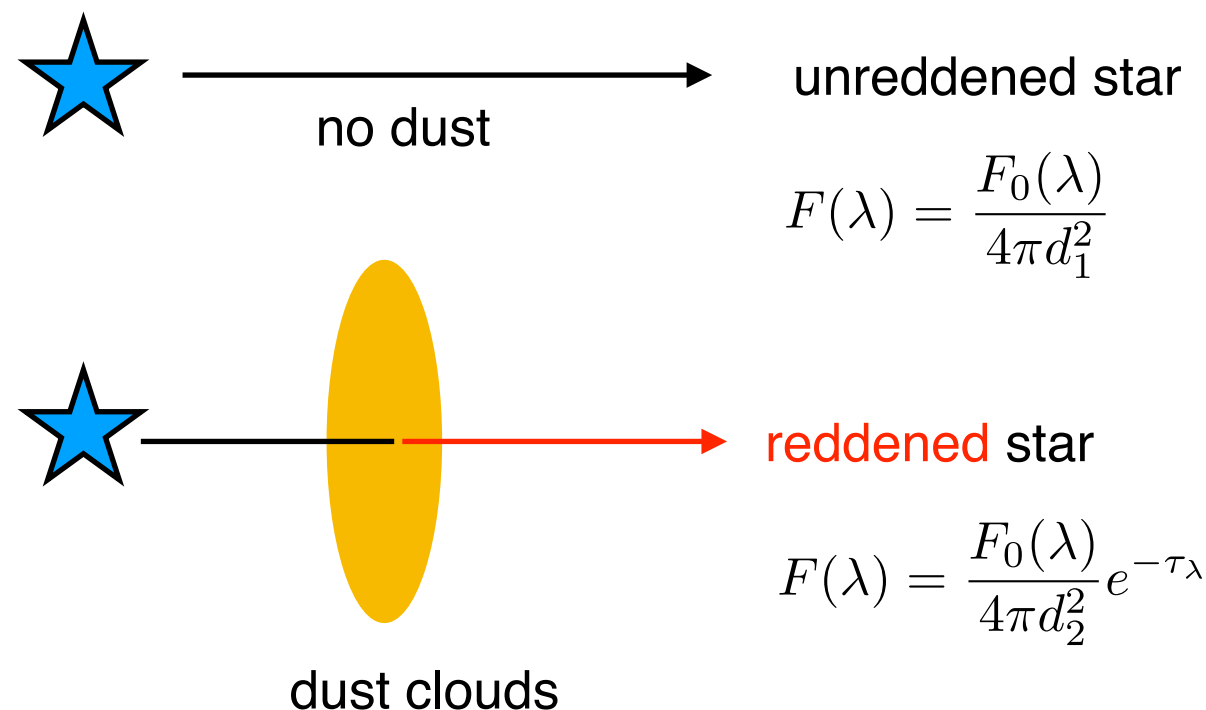
- Given the typical size of interstellar dust grains, blue light is scattered more than red light. ***A reflection nebulae is typically blue*** (so for the same reason that the sky is blue, except it's scattering by dust (for the reflection nebula) vs by molecules (for the earth's atmosphere)).



How to measure the Interstellar Extinction

- Pair method
 - Trumpler (1930) compared the spectra of pairs of stars with identical (or similar) spectral type, one with negligible obscuration and the other extinguished by dust along the line of sight. This method remains our most direct way to study the “selective extinction” or “reddening” of starlight by the interstellar dust.

Compare two stars
with the same spectral type



• ***The Reddening Law, Extinction Curve***

- Extinction curve - the extinction A_λ as a function of wavelength or frequency
 - ▶ A typical extinction curve shows the ***rapid rise in extinction in the UV***.
 - ▶ ***The extinction increases from red to blue***, and thus the light reaching us from stars will be “reddened” owing to greater attenuation of the blue light.
 - ▶ The reddening by dust is expressed in terms of a ***color excess***; for instance,

B-V color excess:

$$E(B - V) \equiv A_B - A_V$$

$\lambda_B \sim 4400 \text{ \AA}$
 $\lambda_V \sim 5500 \text{ \AA}$

in general,

$$E(\lambda_1 - \lambda_2) \equiv A_{\lambda_1} - A_{\lambda_2} \quad (\lambda_1 < \lambda_2)$$

- ▶ The detailed wavelength dependence of the extinction - the “***reddening law***” - is sensitive to the ***composition*** and ***size distribution*** of the dust particles.
- ▶ The slope of the extinction at visible wavelengths is characterized by the dimensionless ratio, ***the ratio of total to selective extinction***:

$$R_V \equiv \frac{A_V}{A_B - A_V} \equiv \frac{A_V}{E(B - V)}$$

- ▶ R_V ranges between 2 and 6 for different lines of sight. Sightlines through diffuse gas in the Milky Way have $R_V \approx 3.1$ as an average value. ***Sightlines through dense regions tend to have larger values of R_V*** . In dense clouds, the value $R_V \approx 5$ is typically adopted.

- ▶ ***Observed extinction curves vary in shape from one line of sight to another.***
- ▶ Extinction curve, relative to the extinction in the I band ($\lambda = 8020\text{\AA}$), as a function of inverse wavelength, for Milky Way regions characterized by different values of R_V .

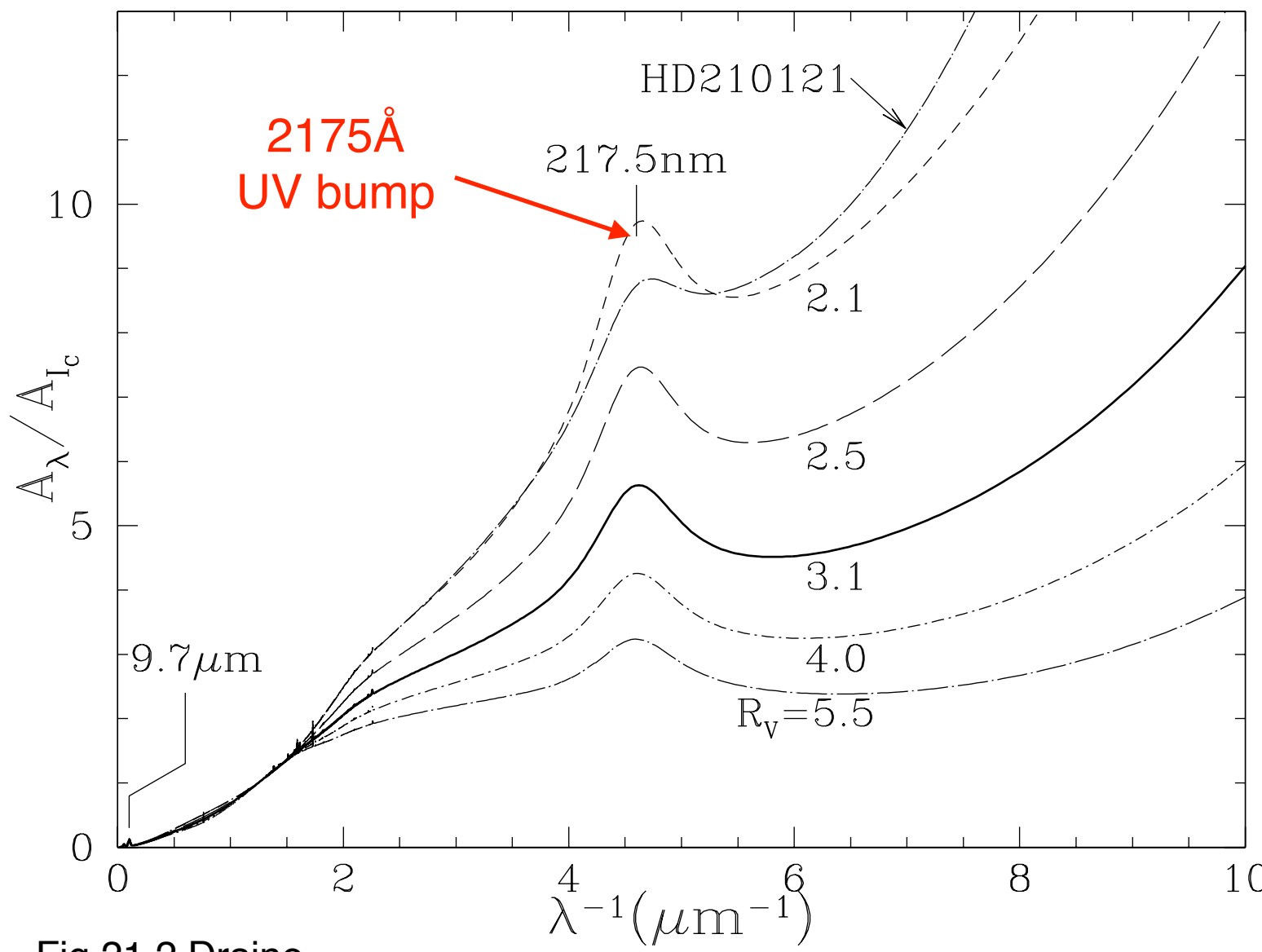


Fig 21.2 Draine

Parameterization of the extinction curve.

Cardelli et al. (1989)

Fitzpatrick (1999)

Gas-to-dust ratio

- If the dust grains were large compared to the wavelength, we would be in the “geometric optics” limit, and the extinction cross section would be independent of wavelength (gray extinction).
 - ▶ The tendency of the extinction to rise with decreasing λ , even at the shortest ultraviolet wavelengths tells us that grains smaller than the wavelength must be making an appreciable contribution to the extinction at all observed wavelengths, down to $\lambda = 0.1 \mu\text{m}$.
 - ▶ According to the Mie theory, “small” means (approximately) that $2\pi a/\lambda \lesssim 1$. Thus interstellar dust must include a large population of small grains with $a \lesssim 0.015 \mu\text{m}$.
- The dust appears to be relatively well-mixed with the gas (Bohlin et al. 1978; Rachford et al. 2009):

$$\frac{N_{\text{H}}}{E(B-V)} = 5.8 \times 10^{21} \text{ H cm}^{-2} \text{ mag}^{-1}$$

Gas-to-dust ratio $\approx 100 - 200$ by mass

- ▶ For sightlines with $R_V \approx 3.1$, this implies that

$$\frac{A_V}{N_{\text{H}}} \approx 5.3 \times 10^{-22} \text{ mag cm}^2 \text{ H}^{-1}$$

column density of total hydrogen nuclei
 $N_{\text{H}} \equiv N(\text{HI}) + 2N(\text{H}_2)$

- ▶ Thus, even at high galactic latitudes, where the column density of hydrogen is $\sim 10^{20} \text{ cm}^{-2}$, there is still some foreground extinction when looking at extragalactic sources; ~ 0.05 magnitudes in the V band.

- ***Mean ratio of visual extinction to length in the Galactic plane***

$$\left\langle \frac{A_V}{L} \right\rangle \approx 1.8 \text{ mag kpc}^{-1}$$

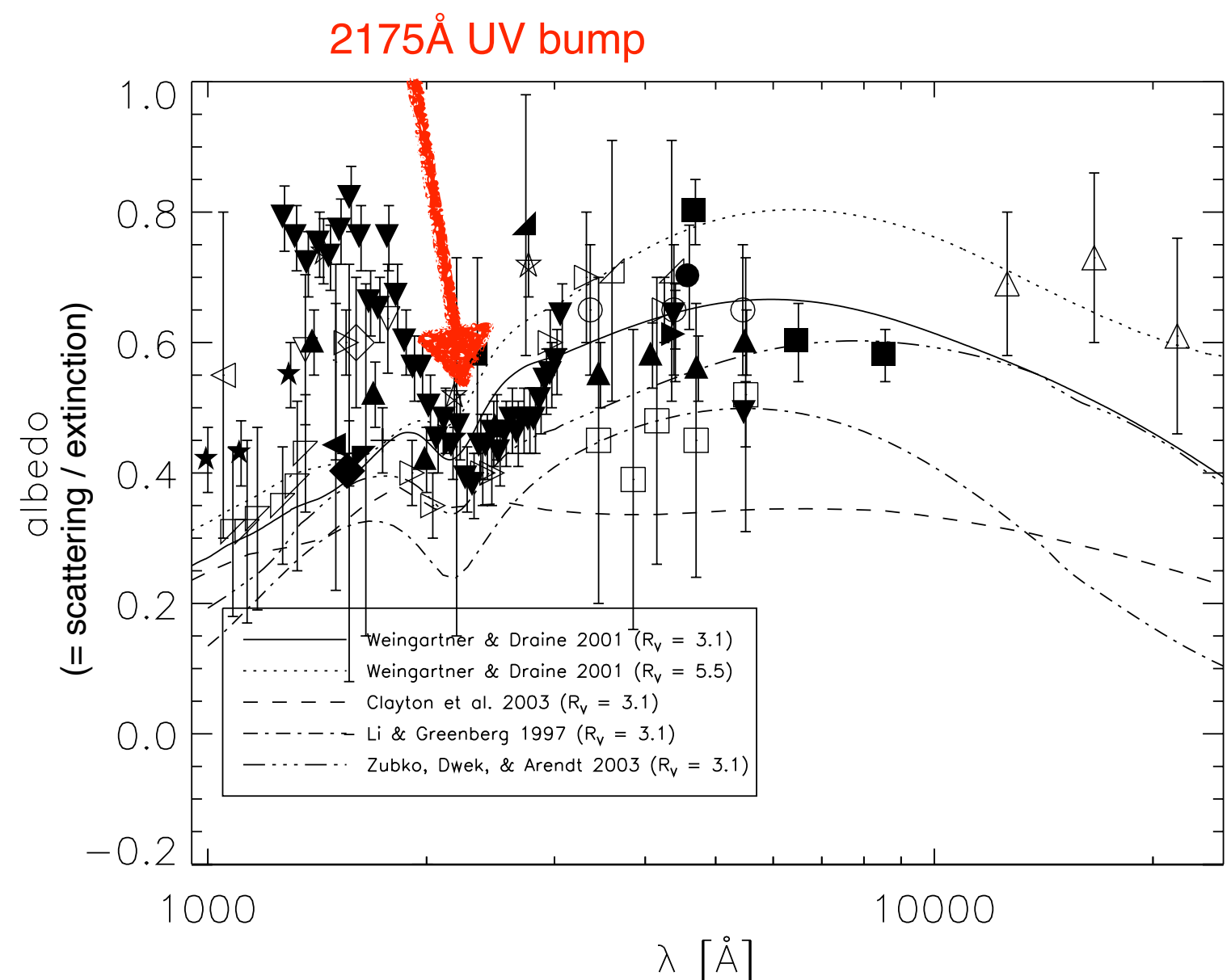
UV bump

- The study of dust scattering properties has shed light on the nature of the 2175Å bump and the far-ultraviolet rise features of extinction curves.
- Lillie & Witt (1976) and Calzetti et al. (1995) showed that ***the 2175Å bump was likely an absorption feature with “no scattering component.”***

The determinations of the albedo in reflection nebulae, dark clouds, and the diffuse Galactic light are plotted versus wavelength.

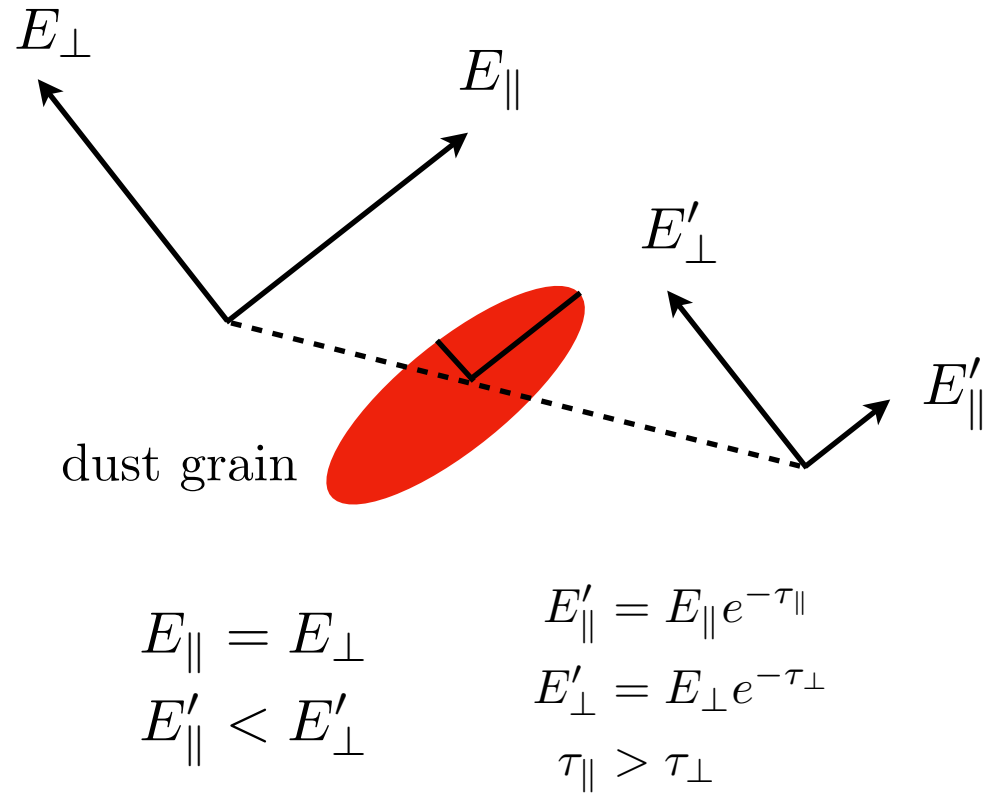
Predictions from dust grain models are also plotted for comparison.

Karl D. Gordon (2004, ASPC, 309, 77)



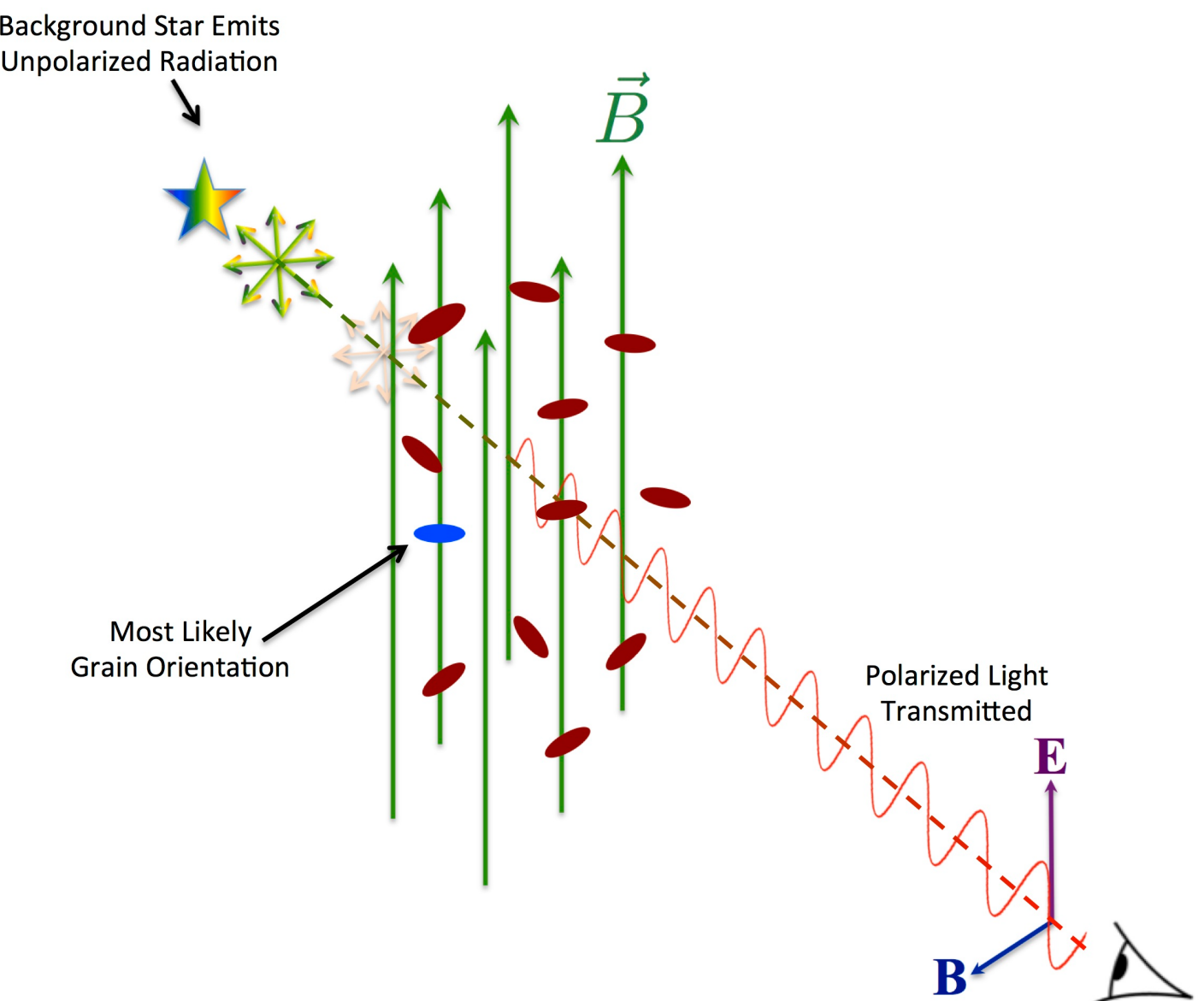
- **Polarization of Starlight by Interstellar Dust**

- Initially unpolarized light propagating through the ISM becomes linearly polarized as a result of ***preferential extinction*** of one linear polarization mode relative to the other.



The starlight is slightly more blocked along the long axis of the grains than along the short axis.

This give rise to the polarization of starlight along the short axis.



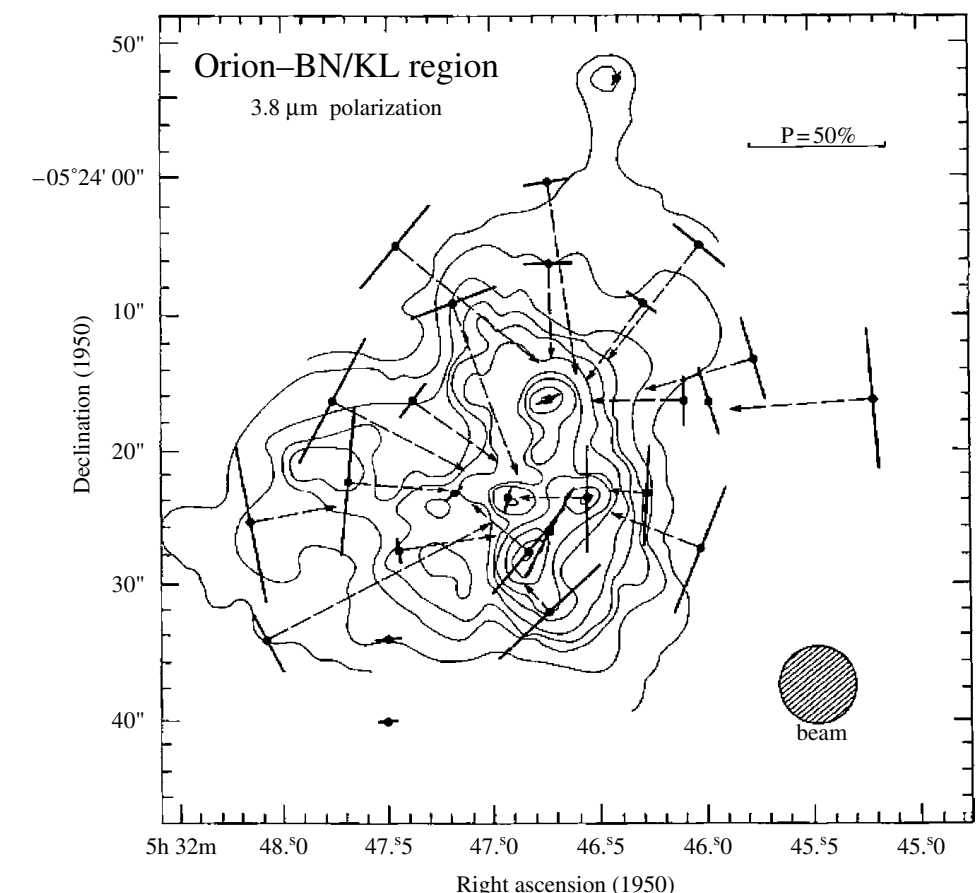
credit: B-G Andersson

- **Polarized Infrared Emission**

- The far-IR emission from aligned dust grains will also be polarized, this time **with a direction along the long axis of the grains**. Far-IR polarization has been observed for a large number of molecular clouds that have “high” dust emission optical depths at long wavelengths ($\sim 0.1\text{-}1$ mm).

- **Polarization due to scattering**

- Scattering of light by dust grains generally also lead to polarization.
- For single scattering, **the polarization vector is perpendicular to the line connecting the light source and the scattering grain**.
- The degree of polarization and its distribution provide information on the characteristics of the scattering grains and the geometry of the nebula.



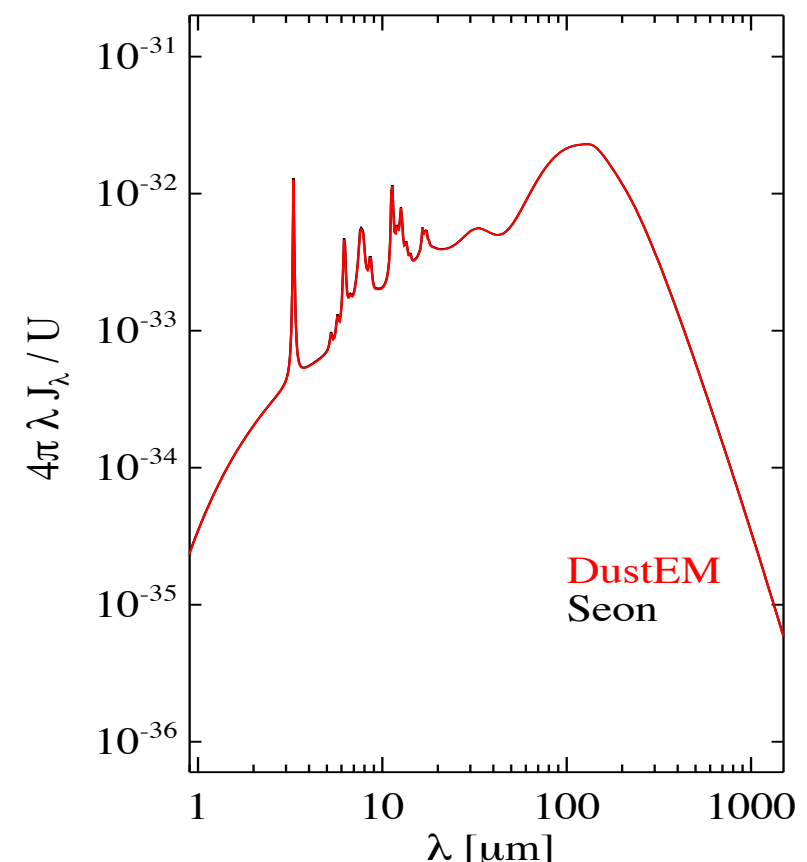
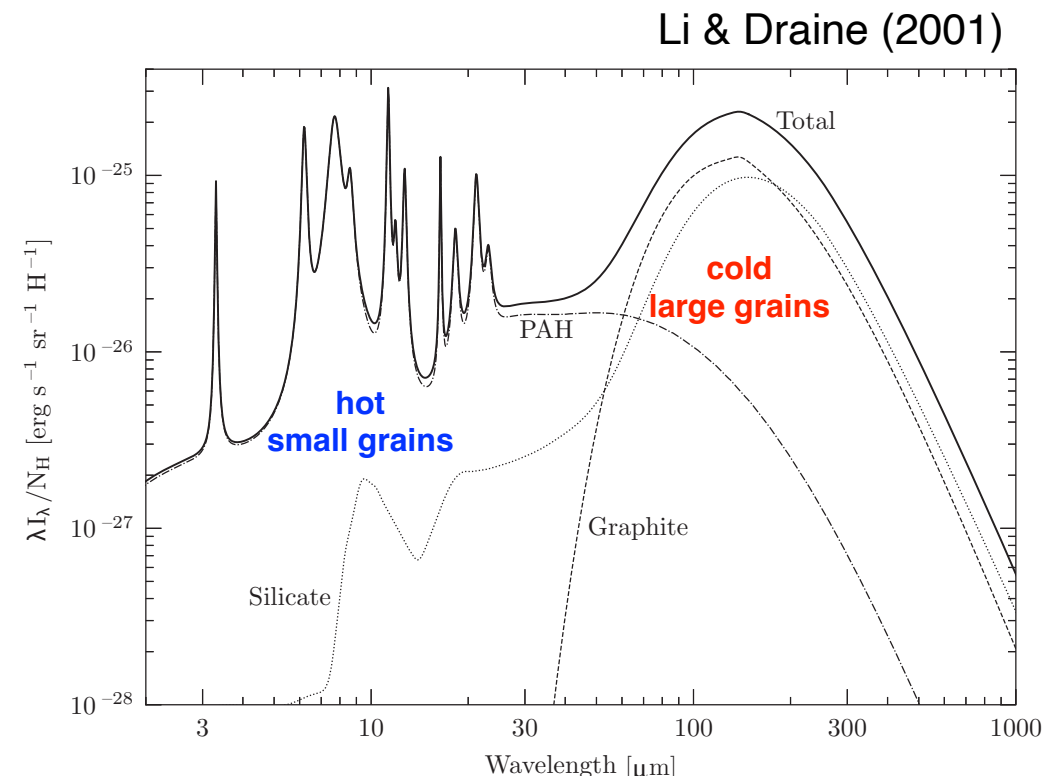
Linear polarization of the IR reflection nebula associated with the region of massive star formation in Orion.
The linear polarization vectors measured at K are superimposed on a map of the scattered light intensity.

[Werner et al. 1983, ApJ, 265, L13]

Infrared Emission

- ***Infrared Emission***

- Dust grains are heated by starlight, and cool by radiating in the infrared.
- The IR spectrum provides very strong constraints on grain models.
- There are two components: ***a cold ($T \sim 15\text{-}20\text{ K}$) component*** emitting mainly at long wavelengths (far-IR) and ***a hot ($T \sim 500\text{ K}$) component*** dominating the near- and mid-IR emission.
 - ▶ The **cold component** is due to **large dust grains** in radiative equilibrium with the interstellar radiation field.
 - ▶ The **hot component** is due to **ultra small grains** and **PAH species** that are heated by a single UV photon to temperatures of $\sim 1000\text{ K}$ and cool rapidly in the near- and mid-IR.



What are the dust grains made of?

- Observational Constraints
 - **Interstellar Depletion:** Certain elements appear to be underabundant or “depleted” in the gas phase. The observed depletions tell us about the major elemental composition of interstellar dust.
 - **Spectroscopy:** We would observe spectroscopic features that would uniquely identify the materials, and allow us to measure the amounts of each material present. But, it is difficult to apply this approach to solid materials because: (1) the optical and UV absorption is largely a continuum; and (2) the spectral features are broad, making them difficult to identify conclusively.
 - **Extinction:**
 - ▶ The wavelength dependence of the extinction curve provides constraints on the interstellar grain size distribution.

Interstellar Depletion

- Condensable elements:
 - ▶ Hydrogen: There is no way to have hydrogen contribute appreciably to the grain mass (even polyethylene (CH_2)_n is 86% carbon by mass).
 - ▶ The noble gases (He, Ne, Ar, Kr, Xe...) and nitrogen(N), zinc (Zn), and sulfur (S) are examples of species that generally form only rather volatile (휘발성) compounds. They are observed to be hardly depleted at all. **volatile = easily evaporated at normal temperature**
 - ▶ The grains are likely to be built out of the most abundant condensable elements: C, O, Mg, Si, S, and Fe (refractory materials; 내열성물질). **refractory = stubborn or unmanageable**
- Abundance Constraints toward ζ Oph
 - ▶ Nitrogen is present at its solar abundance.
 - ▶ C abundance is at $\sim 35\%$ of its solar value.
 - ▶ O abundance is at $\sim 55\%$ of its solar value.
 - ▶ Mg is at $\sim 11\%$.
 - ▶ Si is at $\sim 5\%$.
 - ▶ Fe is at $\sim 0.4\%$.

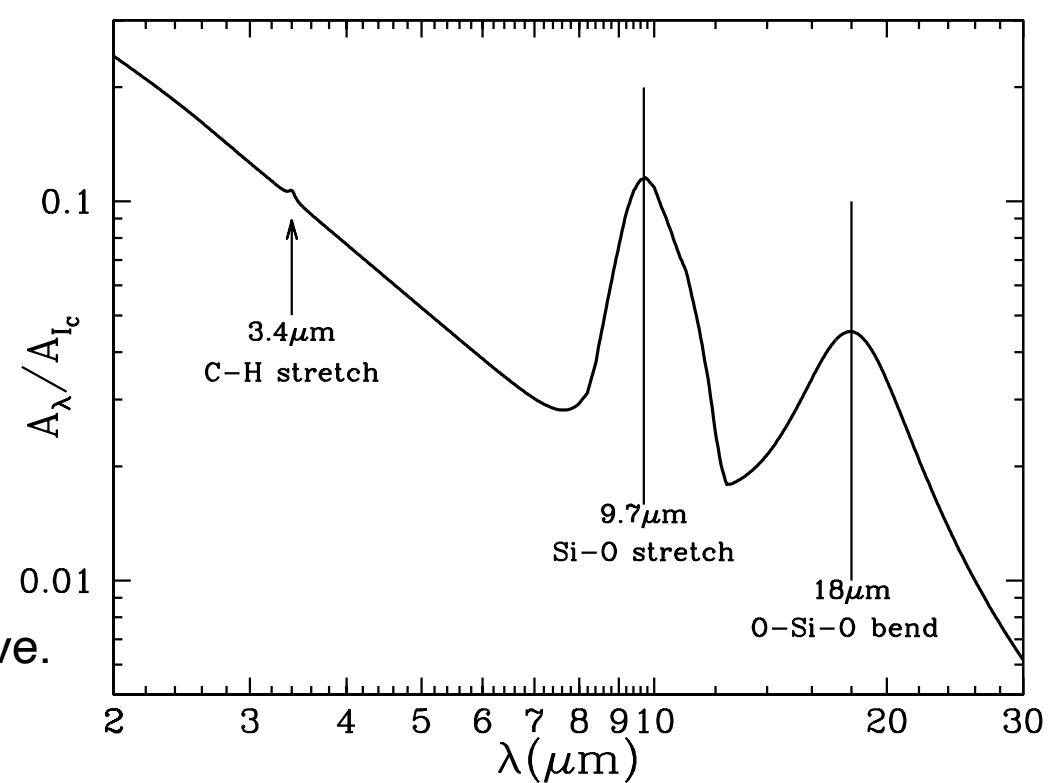
Observed Spectral Features of Dust

- The 2175Å Feature (UV bump)
 - The strongest feature in the interstellar extinction curve is a broad “bump” centered at $\sim 2175\text{\AA}$ where there is additional absorption above the rough $1/\lambda$ behavior at adjacent wavelengths.
 - ▶ The feature is well-described by a **Drude profile**.
 - $$S(\lambda) = \frac{2}{\pi} \frac{\gamma_0 \lambda_0 \sigma_{\text{int}}}{(\lambda/\lambda_0 - \lambda_0/\lambda)^2 + \gamma_0^2} \quad \text{where } \sigma_{\text{int}} = \int S(\lambda) d\lambda^{-1}$$
 - ▶ The central wavelength is nearly identical on all sightlines, but the width varies significantly from one region to another.
 - ▶ The strength of the feature is a strong function of the metallicity of the gas, with the UV bump appearing slightly weaker in the LMC extinction curve (metallicity $\sim 50\%$ solar), but essentially absent in the SMC extinction curve (metallicity $\sim 10\%$ solar).
- The strength of this feature implies that the responsible material must be abundant.

- Mid-Infrared Silicate Features:

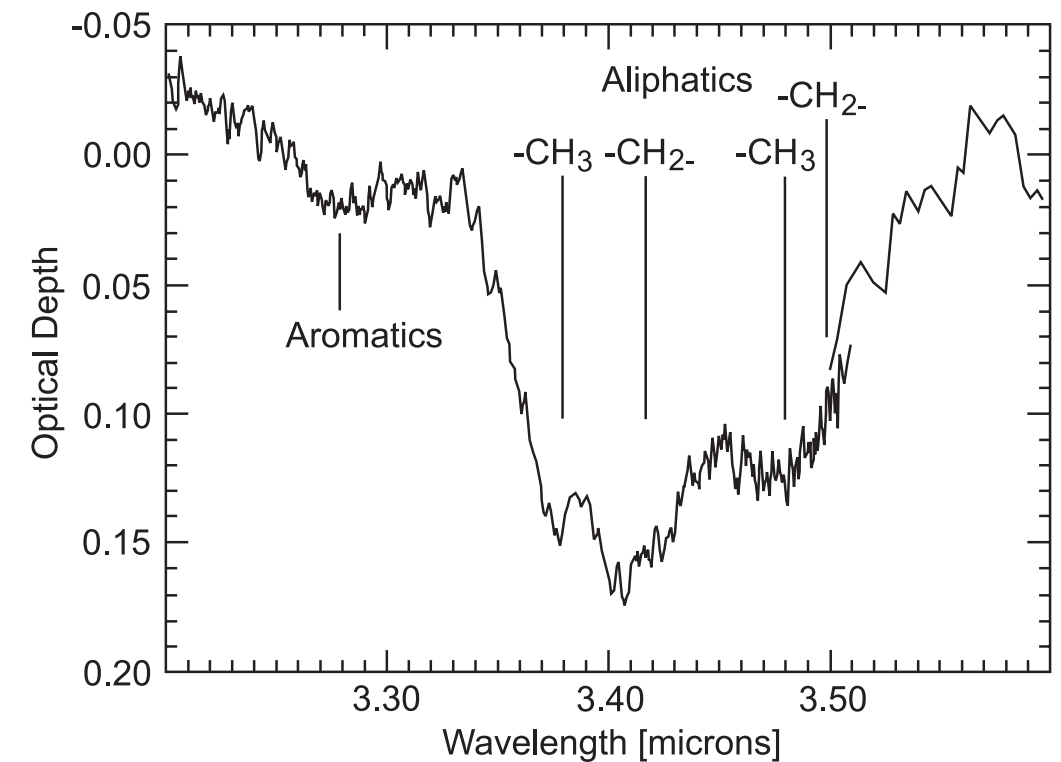
The fact that the $9.7\mu\text{m}$ band is fairly featureless, unlike what is seen in laboratory silicate crystals, suggests that this “astrophysical” silicate is primarily amorphous rather than crystalline in nature.

IR extinction curve.
[Fig 23.2 Draine]



- The $3.4\mu\text{m}$ Feature

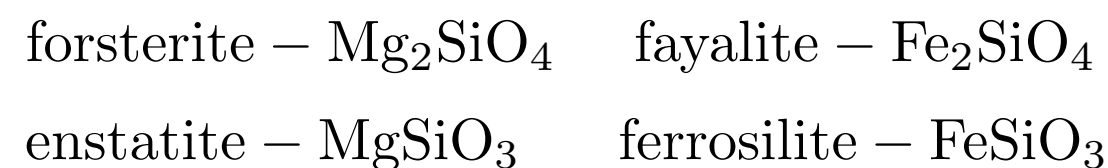
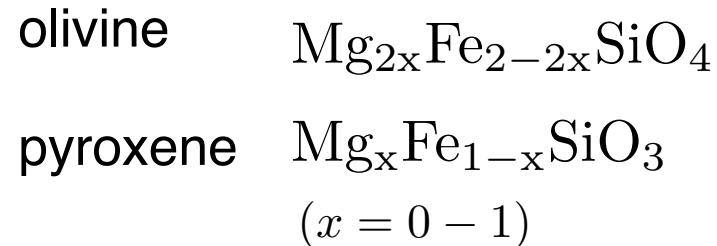
- There is a broad absorption feature at $3.4\mu\text{m}$ that is almost certainly due to the C-H stretching mode in “aliphatic” hydrocarbons (organic molecules with carbon atoms joined in straight or branched chains).



The source GCS3 in the Galactic Center
Chiar et al. (2000, ApJ)

Dust Materials

- Silicates
 - The two main types of silicates in dust are pyroxene and olivine.



[Left] Olivine is the simplest silicate structure, which is composed of isolated tetrahedra bonded to iron and/or magnesium ions. No oxygen atom is shared to two tetrahedra.

[Middle] In pyroxene, silica tetrahedra are linked together in a single chain, where one oxygen ion from each tetrahedra is shared with the adjacent tetrahedron.

[Right] Other types are possible. In amphibole structures, two oxygen ions from each tetrahedra are shared with the adjacent tetrahedra.

In mica structures, the tetrahedra are arranged in continuous sheets, where each tetrahedron shares three oxygens with adjacent tetrahedra.

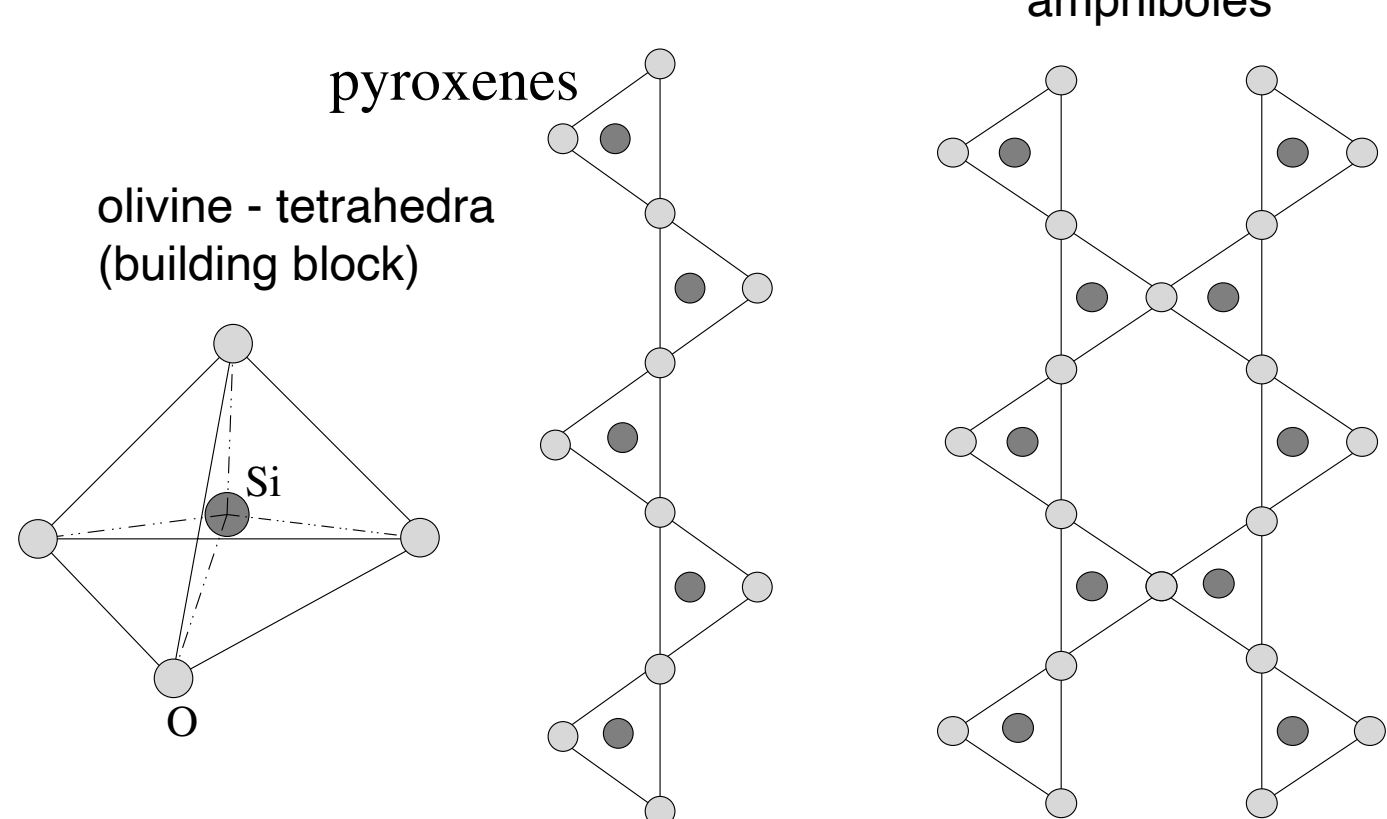
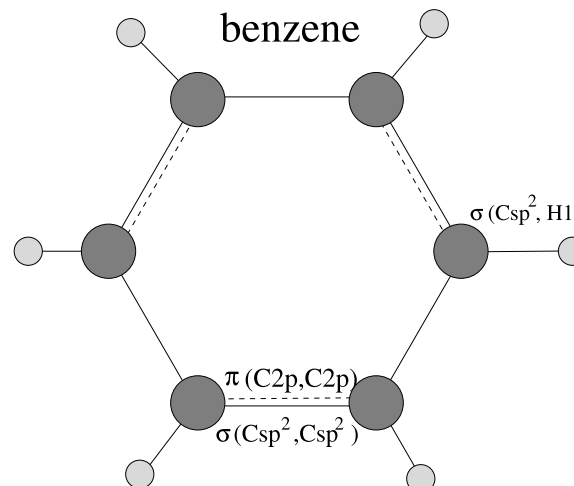


Fig 5.9 Krugel
[An Introduction to the Physics of Interstellar Dust]

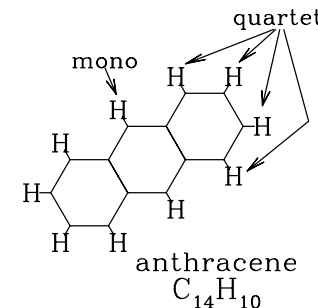
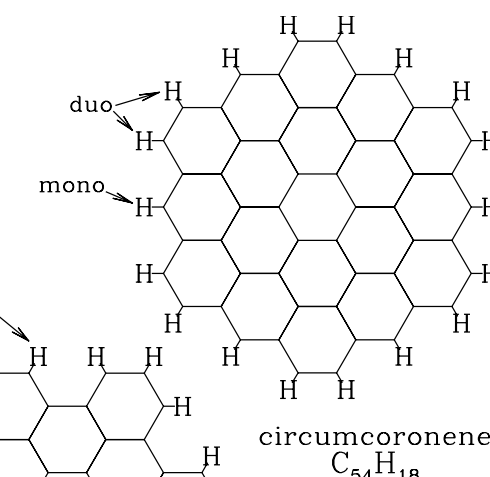
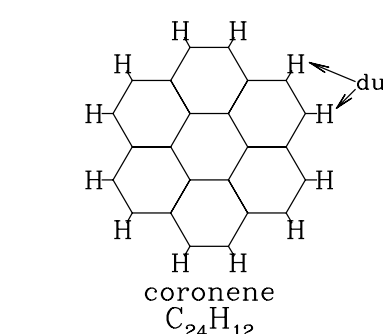
• Polycyclic Aromatic Hydrocarbons (PAHs)

- The IR emission spectra of spiral galaxies show emission features at 3.3, 6.2, 7.7, 8.6, 11.3, and 12.7 μm that are attributable to vibrational transitions in polycyclic aromatic hydrocarbon (PAH) molecules.
- PAH molecules are planar structures consisting of carbon atoms organized into hexagonal rings, with hydrogen atoms attached at the boundary.

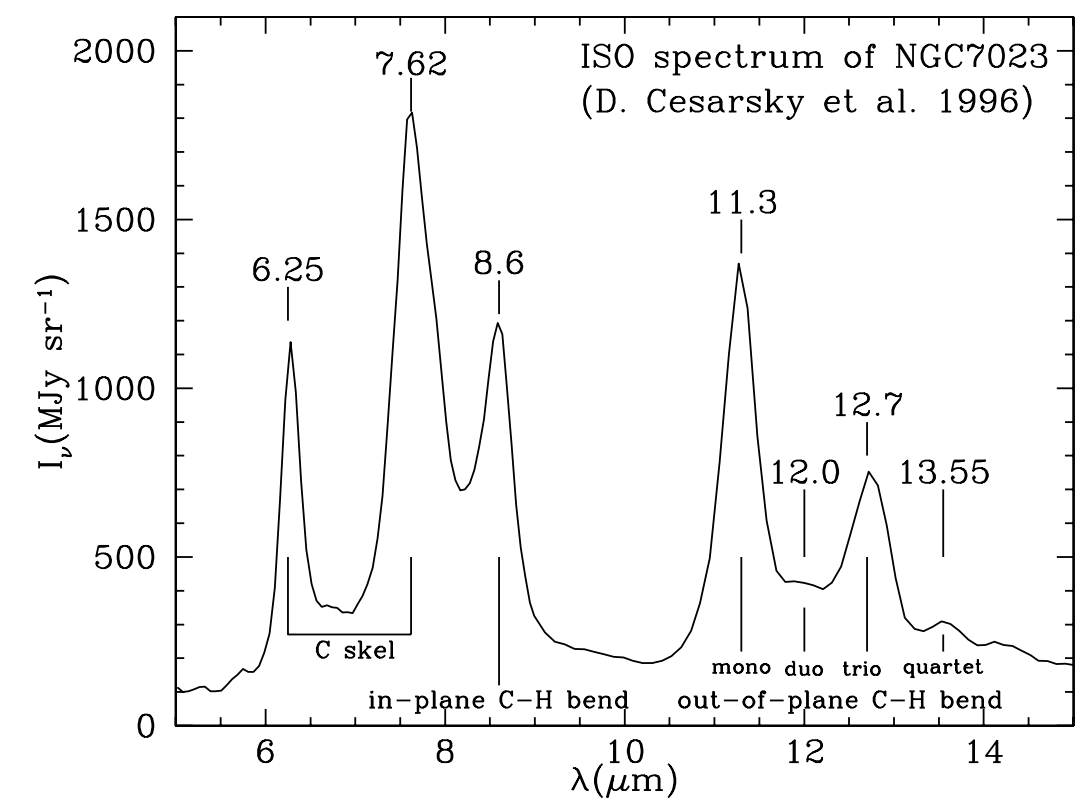


Bezene ring:
The simplest type of PAHs.

[Fig 5.6 in Krugel]



Structure of four PAHs.
[Fig 23.9 in Draine]



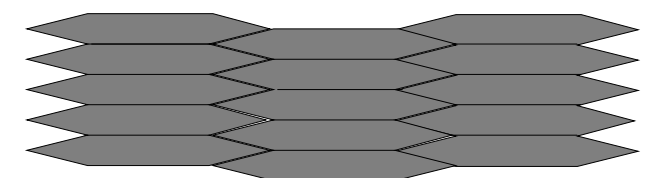
The IR spectrum of the reflection nebula NGC 7023 (Cesarsky et al. 1996)

- Graphite (흑연)

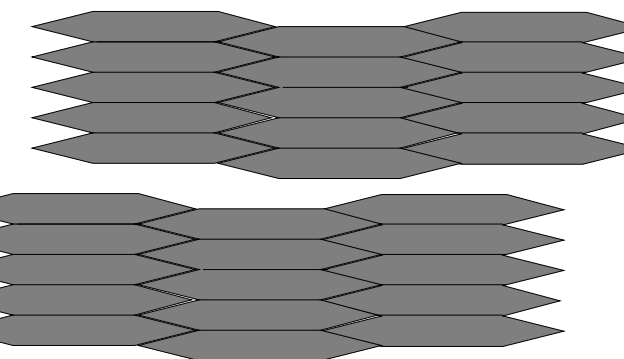
- Graphite is the most stable form of carbon (at low pressure), consisting of infinite parallel sheets of sp^2 -bonded carbon.
 - ▶ A single (infinite) sheet of carbon hexagons is known as graphene. Each carbon atom in graphene has three nearest neighbors, with a nearest-neighbor distance of 1.421\AA .
 - ▶ Crystalline graphite consists of regularly stacked graphene sheets.
 - ▶ The sheets are weakly bound to one another by van der Waals forces.



graphite sheets

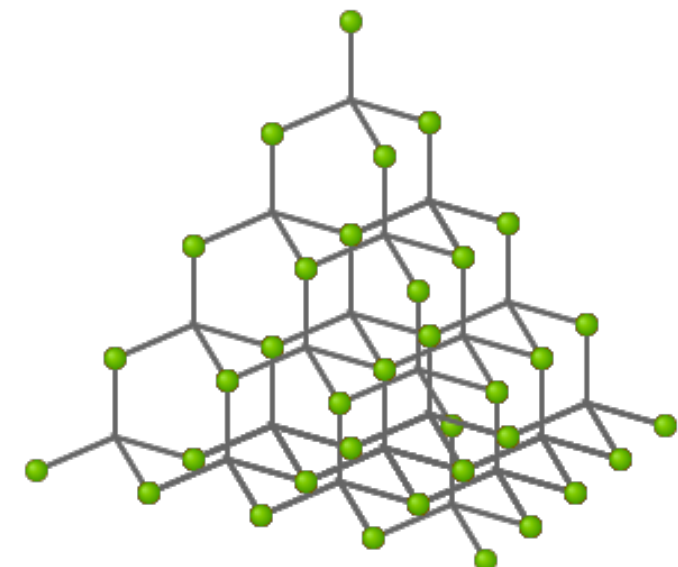


3.35\AA



- Nanodiamond

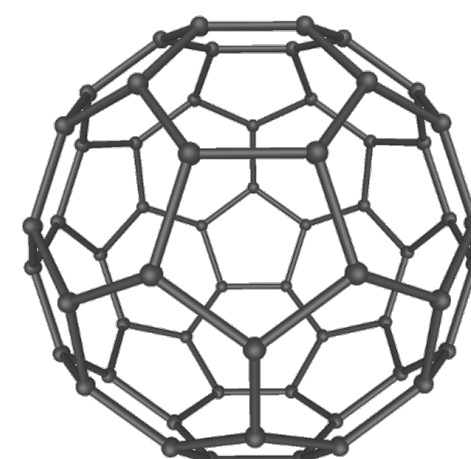
- Diamond consists of sp^3 -bonded carbon atoms, with each carbon bonded to four equidistant nearest neighbors (enclosed angles are 109.47°).
- Diamond nanoparticles are relatively abundant in primitive meteorites. Based on isotopic anomalies associated with them, we know that some fraction of the nanodiamond was of premolar origin.
- But, its abundance in the ISM is not known.



- Armorphous carbon

- Hydrogenated amorphous carbon (HAC)

- Fullerenes



Buckminsterfullerene (C_{60})

Structure of diamond.

Dust Theory: cross section and efficiency factors

- **Cross Sections:**

- A dust grain has wavelength-dependent cross sections for absorption and scattering.
Extinction is the sum of absorption and scattering processes.

$$C_{\text{ext}}(\lambda) = C_{\text{abs}}(\lambda) + C_{\text{sca}}(\lambda)$$

- For a population of dust grains with number density n_d , the extinction cross section is related to the extinction coefficient and the dust optical depth by:

$$\begin{aligned}\kappa_\lambda &= n_d C_{\text{ext}}(\lambda) \\ \tau_\lambda &= n_d C_{\text{ext}}(\lambda) L \quad L = \text{pathlength} \\ &= 1.086 A_\lambda\end{aligned}$$

- **Efficiency Factors:**

- The cross section is often expressed in terms of efficiency factors, normalized to the geometric cross section of an equal-solid-volume sphere:

$$Q_{\text{ext}}(\lambda) = \frac{C_{\text{ext}}(\lambda)}{\pi a^2}, \quad Q_{\text{abs}}(\lambda) = \frac{C_{\text{abs}}(\lambda)}{\pi a^2}, \quad Q_{\text{sca}}(\lambda) = \frac{C_{\text{sca}}(\lambda)}{\pi a^2}$$

$$V = \frac{4\pi}{3} a^3 \quad a = \text{the radius of an equal-volume sphere}$$

- Albedo and Scattering phase function
 - The **albedo** (for a single scattering) is defined by

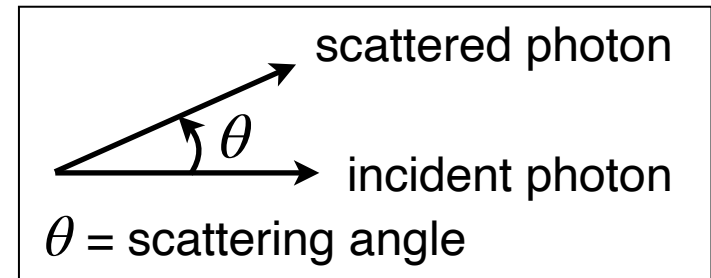
$$\omega(\lambda) = \frac{C_{\text{sca}}(\lambda)}{C_{\text{ext}}(\lambda)} = \frac{C_{\text{sca}}(\lambda)}{C_{\text{abs}}(\lambda) + C_{\text{sca}}(\lambda)}$$

In many cases, the albedo is denoted by a or ω .

- The scattering phase function (probability density function) can be described by the Rayleigh function or Henyey-Greenstein function:

$$\mathcal{P}_{\text{Ray}}(\theta) = \frac{1}{2} (1 + \cos^2 \theta) \quad \text{for } \frac{2\pi a}{\lambda} \ll 1 \longrightarrow \langle \cos \theta \rangle = 0$$

$$\mathcal{P}_{\text{HG}}(\theta) = \frac{1}{2} \frac{1 - g^2}{(1 + g^2 - 2g \cos \theta)^{3/2}} \quad \text{for } \frac{2\pi a}{\lambda} \gg 1 \longrightarrow \langle \cos \theta \rangle = g$$



- ▶ The Henyey-Greestein phase function is only introduced for computational convenience and has no physical meaning.
- The **scattering asymmetry factor** is defined by:

$$g \equiv \langle \cos \theta \rangle = \int_0^{2\pi} \int_0^\pi \cos \theta \mathcal{P}(\cos \theta) \sin \theta d\theta d\phi$$

| | |
|-----------------------|--------------------------------------|
| $g \approx 0.6 - 0.7$ | forward scattering in the UV/optical |
| $g \approx 0$ | ~ isotropic in IR |

Theoretical Model of the Extinction Curve

- Scattering Theory: How to calculate the theoretical extinction curve.
 - **Mie scattering** (Gustave Mie), the general solution for (absorbing or non-absorbing) spherical particles without a particular bound on particle size. ==> complex
- A model for interstellar dust must specify the **composition** of the dust as well as the geometry (**shape and size**) of the dust particles.
 - If the model is to reproduce the polarization of attenuated starlight, at least some of the grains should be nonspherical and aligned.
 - However, it is not yet possible to arrive at a unique grain model.

Models for Interstellar Dust

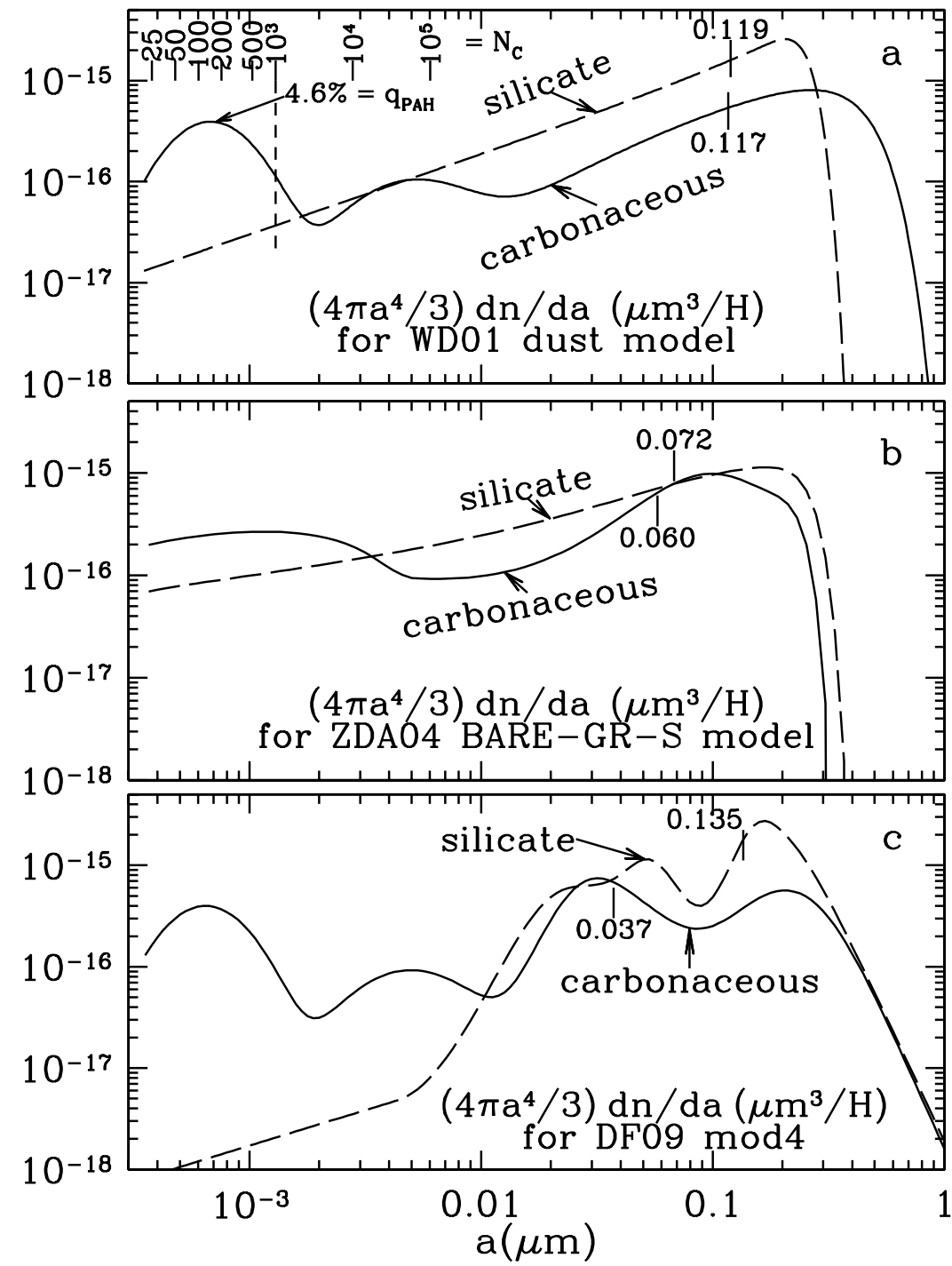
- A class of models that has met with some success assumes the dust to consist of two materials: **(1) amorphous silicate, and (2) carbonaceous material.**
 - ***Mathis, Rumpl, and Nordsieck (1977; MRN)*** found that models using two components, silicate and graphite spheres with power-law size distributions, could reproduce the observed extinction from the near-IR to the UV ($\lambda = 0.11\mu\text{m} - 1\mu\text{m}$).

$$\frac{dn_{\text{gr}}}{da} da = A_i n_{\text{H}} a^{-3.5} da \quad \text{for } a_{\min} \leq a \leq a_{\max}$$

$a_{\min} \approx 0.025\mu\text{m}$
 $a_{\max} \approx 0.25\mu\text{m}$

$$A_{\text{sil}} = 7.8 \times 10^{-26}, \quad A_{\text{gra}} = 6.9 \times 10^{-26} \text{ cm}^{2.5} (\text{H atom})^{-1}$$

- ▶ Graphite was a necessary component. The other could be silicon carbide (SiC), magnetite (Fe_3O_4), iron, olivine, or pyroxene.
- ***Draine and Collaborators***
 - ▶ Draine & Lee (1984) presented self-consistent dielectric functions for graphite and silicate, and showed that the graphite-silicate model appeared to be consistent with what was known about dust opacities in the Far-IR. (extended the MRN model to the Far-IR).
 - ▶ Recently, Draine & B. Hensley (2021, ApJ, 909, 94) developed the model composed of the “Astrodust” material, which is a mix of amorphous silicates and other materials. (They does not exist in two different material components, but in a single mixed material.)
- ***Zubko et al. (2004)***
 - ▶ The size distribution of the “BARE-GR-S” model of Zubko et al. (2004), composed of bare graphite grains, bare silicate grains, and PAHs, differs significantly from the WD01 size distribution.



A “typical” grain size may be taken as the half-mass grain size $a_{0.5}$, defined so that half the mass of dust is in grains of radius $a_{0.5}$ or greater.

Size distributions for silicate and carbonaceous grains for dust models from (a) Weingartner & Draine (2001), (b) Zubko et al. (2004), and (c) Draine & Faisse (2009).

In each case, tick-marks indicate the “half-mass” radii for the silicate grains and carbonaceous grains.

[Fig 23.10 Draine]

Temperatures of Interstellar Grains

- The “temperature” of a dust grain is a measure of the internal energy present in **vibrational modes** and possibly also in low-lying electronic excitations.
- Grain Heating
 - In diffuse regions, where ample starlight is present, **grain heating is dominated by absorption of starlight photons.**
 - In dense dark clouds, grain heating can be dominated by inelastic collisions with atoms or molecules from the gas (grain-grain collisions are too infrequent).
- When an optical or UV photon is absorbed by a grain, an electron is raised into an excited electronic state; three cases can occur.
 - If the electron is sufficiently energetic, it may be able to escape from the solid as a **“photoelectron.”**
 - In most solids or large molecules, however, **the electronically excited state will deexcite nonradiatively, with the energy going into many vibrational modes - i.e., heat.**

Temperature of Large Grains and Small Grains

- Large Grains
 - Grains with radii $a \gtrsim 0.03 \mu\text{m}$, can be considered “classical.” These grains are macroscopic - absorption or emission of single quanta do not appreciably change the total energy in vibrational or electronic excitations.
 - The temperature of a large dust grain can be obtained by equating the heating rate to the cooling rate.
- Very Small Grains
 - For ultra-small particles, ranging down to large molecules, quantum effects are important (this include the “spinning” dust grains responsible for microwave emission).
 - When a dust particle is very small, its temperature will fluctuate. This happens because whenever an energetic photon is absorbed, the grain temperature jumps up by some not negligible amount and subsequently declines as a result of cooling.

* Heating & Cooling *

- Radiative Heating rate (for a single particle):
 - the rate of heating of the grain by absorption of radiation can be written.

$$\begin{aligned}\left(\frac{dE}{dt}\right)_{\text{abs}} &= \int \frac{u_\nu d\nu}{h\nu} \times c \times h\nu \times C_{\text{abs}}(\nu) \\ &= \int d\nu 4\pi J_\nu C_{\text{abs}}(\nu)\end{aligned}$$

Here, $u_\nu d\nu/h\nu$ is the number density of photons; the photons move at the speed of light c and carry energy $h\nu$.

- Radiative Cooling rate (for a single particle)

- Kirchhoff's Law in LTE (local thermodynamic equilibrium)

| | |
|--|--|
| $j_\nu = \text{emissivity per unit volume per solid angle}$ | $j_\nu/n_d = \text{emissivity per particle}$ |
| $\kappa_\nu = \text{absorption coefficient per unit length}$ | $\kappa_\nu/n_d = C_{\text{abs}}(\nu) = \text{absorption cross section}$ |
| | $n_d = \text{number density of dust particles}$ |

$$\frac{j_\nu}{\kappa_\nu} = B_\nu(T) \Rightarrow \frac{j_\nu}{n_d} = C_{\text{abs}}(\nu)B_\nu(T)$$

$[B_\nu(T) = \text{Planck function}, \kappa_\nu = n_d C_{\text{abs}}(\nu)]$

- Grains lose energy by infrared emission at a rate:

$$\left(\frac{dE}{dt}\right)_{\text{emiss}} = \int d\nu 4\pi j_\nu/n_d = \int d\nu 4\pi B_\nu(T_d)C_{\text{abs}}(\nu)$$

Equilibrium Temperature

- Steady state temperature of large grains
 - The balance equation between the heating and cooling is:

$$\left(\frac{dE}{dt} \right)_{\text{abs}} = \left(\frac{dE}{dt} \right)_{\text{emiss}}$$

$$\int d\nu J_\nu C_{\text{abs}}(\nu) = \int d\nu B_\nu(T) C_{\text{abs}}(\nu)$$

⇒ calculate the temperature of grains.

- In general, the absorption cross section in the far-IR can be approximated as a power-law in frequency,

$$C_{\text{abs}}(\nu) = C_0 (\nu/\nu_0)^\beta = C_0 (\lambda/\lambda_0)^{-\beta} \quad (1 \lesssim \beta \lesssim 2)$$

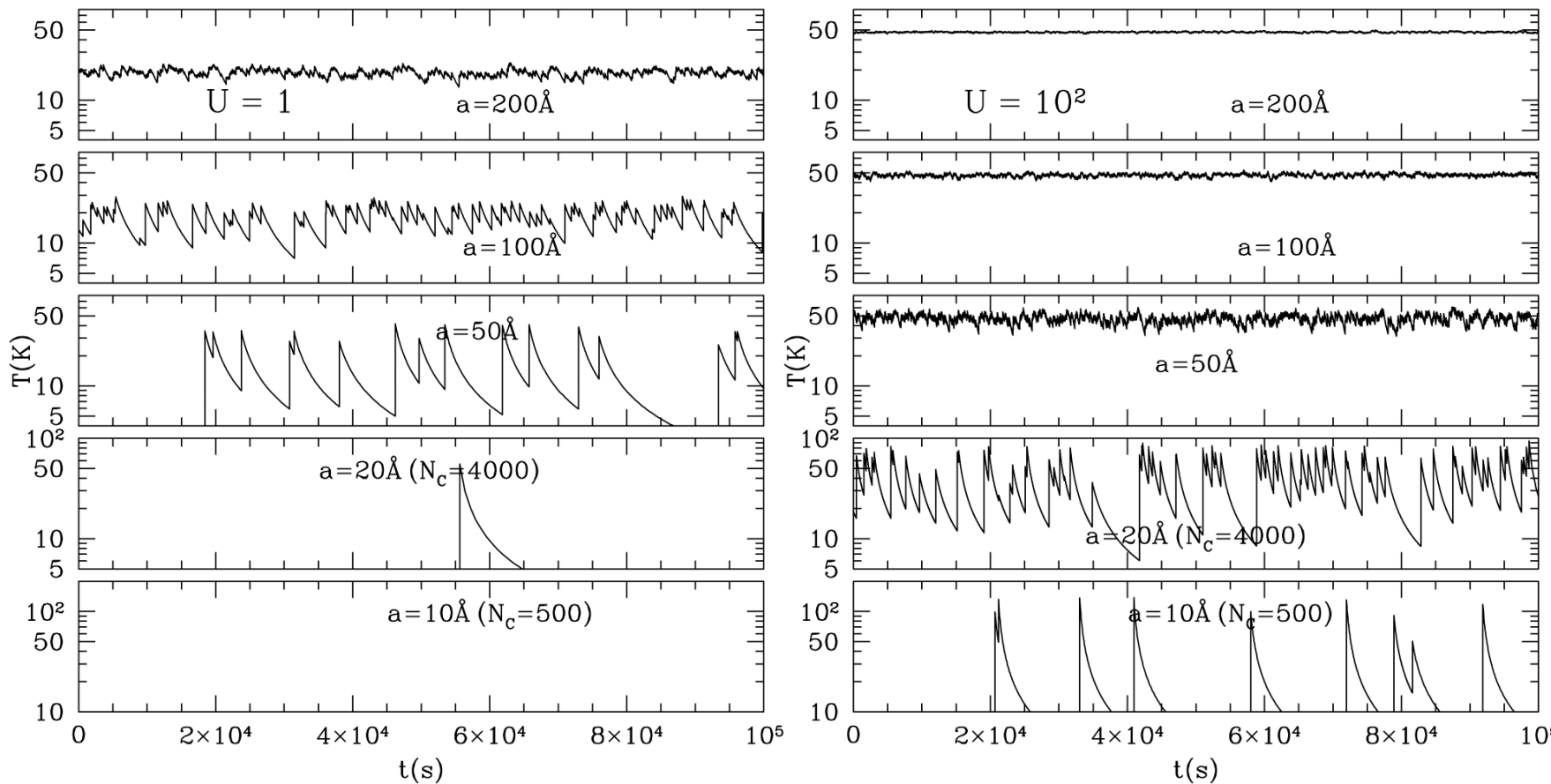
in the far-IR

- ***There is also little dependence of the grain temperature on grain radius. Therefore, large grains can be regarded to be grains with a single size.***

Stochastic Heating of Very Small Grains

- Temperature History:

- ▶ Two effects become increasingly important with diminishing grain size: (1) the heat capacity of the dust becomes sufficiently small that single-particle hits can cause large spikes in the dust temperature and (2) the absorption rate with photons becomes sufficiently low that the cooling of the dust between successive collisions becomes important.
- ▶ ***Therefore, for very small dust grains, it is clear that one cannot speak of a representative grain temperature under these conditions - one must instead use a temperature distribution function.***



Monte-Carlo simulations of the temperature fluctuation:

Temperature versus time during 10^5 s (~ 1 day) for five carbonaceous grains in two radiation fields: the local starlight intensity ($U = 1$; left panel) and 10^2 times the local starlight intensity ($U = 10^2$; right panel). The importance of quantized stochastic heating is evident for the smallest sizes.

[Fig 24.5, Draine]

Formation of Stars

Star-Gas-Star Cycle

- Stars (and their planetary systems) are formed out of the ISM material through gravitational contraction, making for a kind of star-gas-star cycle.

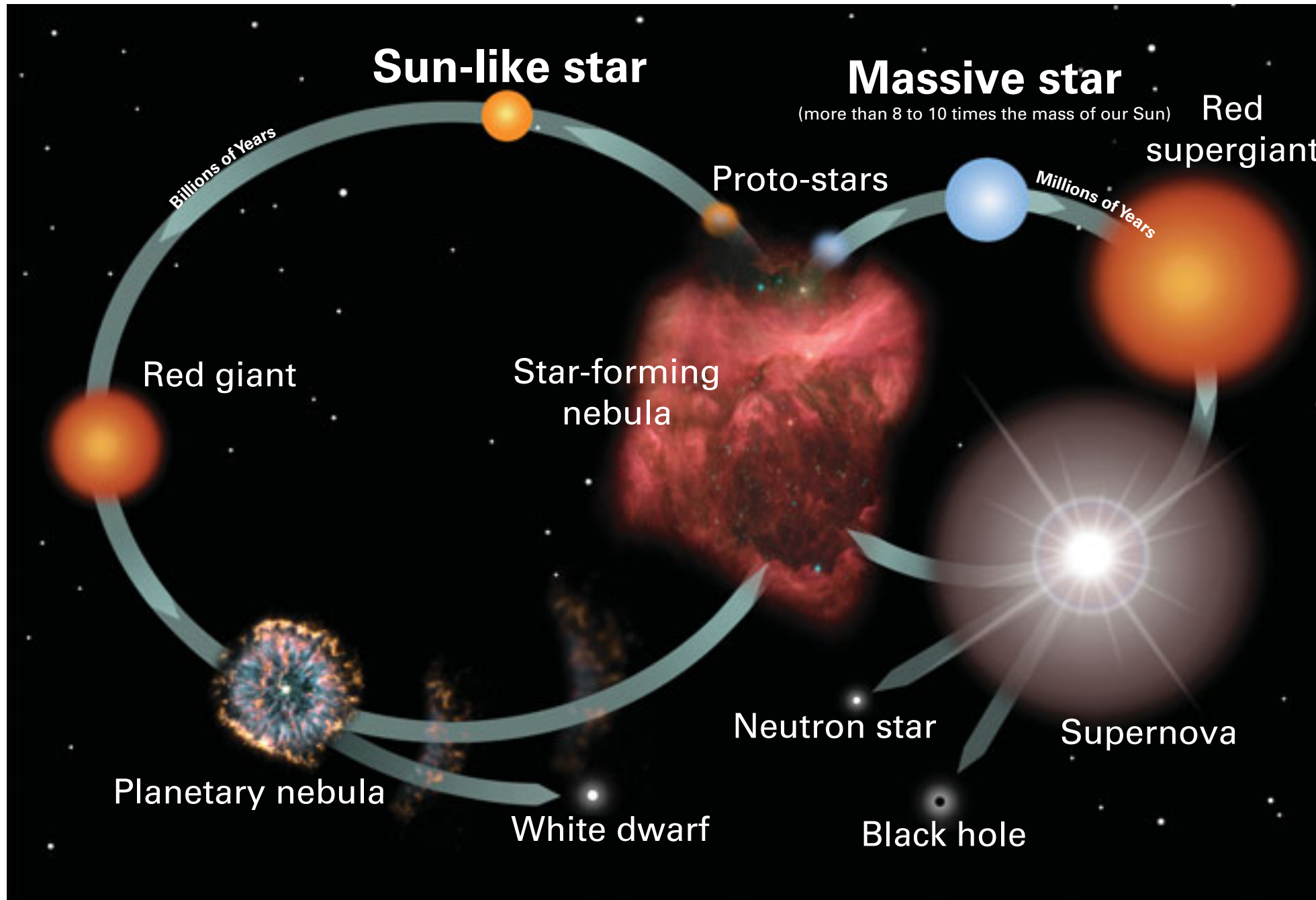


Illustration of formation of solar-type and massive stars from interstellar cloud [S. Owocki]

Virial Theorem

- The virial theorem is a relation between the total kinetic energy and the total gravitational potential energy of a stable bound systems, .i.e., **systems that hang together forever and whose parameters** (such as velocities and coordinates of the particles) are finite.
 - The virial theorem provides a general equation that relates **the average over time of the total kinetic energy** of a stable, self-gravitating system of discrete particles, with **the total gravitational potential energy** of the system.
- See the following reference for the derivation of the virial theorem:
<https://www.uio.no/studier/emner/matnat/astro/nedlagte-emner/AST1100/h09/undervisningsmateriale/lecture5.pdf>

$$2 \langle K \rangle + \langle U \rangle = 0$$

K = kinetic energy

U = gravitational potential energy

Jeans Criterion for Gravitational Contraction

- Stars generally form in clusters from the gravitational contraction of a dense, cold GMC.
 - The requirements for such gravitational contraction depend on the relative magnitudes of the total internal thermal (kinetic) energy K versus the gravitational binding energy U .
 - For a cloud of mass M , uniform temperature T , and mean mass per particle μ , the total number of particles $N = M/\mu$ have an associated total thermal energy,

$$K = \frac{3}{2} N k_B T = \frac{3}{2} \frac{M k_B T}{\mu}$$

- For a spherical cloud with radius R and uniform density, the associated gravitational binding energy is

$$U = -\frac{3}{5} \frac{GM^2}{R}$$

see the reference in the previous page.

- Recall that $K = -U/2$ is the condition for stably bound systems in the virial equilibrium.
 - ◆ Therefore, for a cloud with $K > -U/2$, the excess internal pressure would do work to expand the cloud against gravity, leading to it to be unbound.
 - ◆ Conversely, for $K < -U/2$, the too-low pressure would allow the cloud to gravitationally contract, leading to a more strongly bound cloud.

- The critical requirement, known as the **Jeans criterion**, for gravitational contraction can be obtained from the above argument.

$$K < -U/2 \implies \frac{3}{2} \frac{Mk_B T}{\mu} < \frac{3}{10} \frac{GM^2}{R} \implies \frac{M}{R} > \frac{5k_B T}{G\mu}$$

- **Jeans radius** (in terms of the number density of atom $n = \rho/\mu$)

substituting $M = \frac{4\pi}{3} R^3 n \mu$ $\implies R > \left(\frac{15}{4\pi} \frac{k_B T}{G n \mu^2} \right)^{1/2} \equiv R_J$

molecular hydrogen
↓

$$R > R_J \approx 15 \text{ pc} \left(\frac{T/100 \text{ K}}{n/10 \text{ cm}^{-3}} \right)^{1/2} \left(\frac{2m_p}{\mu} \right)$$

- **Jeans mass**

$$M = \frac{4\pi}{3} R^3 n \mu > \frac{4\pi}{3} R_J^3 n \mu = \frac{5}{\mu^2} \left(\frac{15}{4\pi n} \right)^{1/2} \left(\frac{k_B T}{G} \right)^{3/2} \equiv M_J$$

$$M > M_J \approx 7300 M_{\odot} \frac{(T/100 \text{ K})^{3/2}}{(n/10 \text{ cm}^{-3})^{1/2}} \left(\frac{2m_p}{\mu} \right)^2$$

- For typical ISM conditions, both the Jeans radius and mass are quite large, implying it can be actually quite difficult to initiate gravitational contraction.
- **Jeans fragmentation:**
 - The Jeans length and mass both scale inversely with the square root of the density. This suggests that **a collapsing cloud may break into multiple smaller pieces** as it becomes denser.
 - A general conclusion of such a large Jeans mass is that **stars tend typically to be formed in large clusters, resulting from an initial contraction of a GMC**, with mass of order 10^4 solar mass or more.

Free-fall time (Dynamical time scale)

- **Free-fall timescale**

- In the absence of any support, the collapse can be described as a free-fall with acceleration determined by the gravitational force,

$$m \frac{d^2r}{dt^2} = -\frac{GMm}{r^2} \quad (m = \text{test particle mass})$$

- boundary condition: $v = \frac{dr}{dt} = 0$ at the outer radius $r = R$

$$\frac{d^2r}{dt^2} = \frac{dv}{dr} \frac{dr}{dt} = \frac{1}{2} \frac{dv^2}{dr} \longrightarrow \frac{dv^2}{dr} = -\frac{GM}{r^2} \implies v^2 = 2GM \left(\frac{1}{r} - \frac{1}{R} \right) \implies \frac{dr}{dt} = -\left[2GM \left(\frac{1}{r} - \frac{1}{R} \right) \right]^{1/2}$$

$$\int_0^{t_{ff}} dt = - \int_R^0 \frac{dr}{\left[2GM \left(\frac{1}{R} - \frac{1}{r} \right) \right]^{1/2}} = \left(\frac{2R^3}{GM} \right)^{1/2} \frac{\pi}{4}$$

the negative sign is chosen because the core is collapsing.

- free-fall time (the times for the test particle to move from the outer radius to the center)

$$M = \frac{4}{3}\pi R^3 \rho \rightarrow t_{ff} = \left(\frac{3\pi}{32G\rho} \right)^{1/2} = 3.6 \left(\frac{100 \text{ cm}^{-3}}{n} \right)^{1/2} \left(\frac{2m_p}{\mu} \right)^{1/2} \text{ Myr}$$

- Note that we assumed no force against the gravity. But, there will be a significant source of internal pressure against the gravity while the material collapse.

• Star Formation Efficiency

- In our Galaxy, the total mass in GMCs with density $n \gtrsim 100 \text{ cm}^{-3}$ is $M_{\text{GMC}} \approx 10^9 M_{\odot}$. Since this mass should collapse to stars over a free-fall time, it suggests an overall galactic star-formation rate is given by

$$\dot{M}_{\text{SFR}} = \frac{M_{\text{GMC}}}{t_{\text{ff}}} \approx 280 M_{\odot} \text{ yr}^{-1}$$

- But the observationally inferred star-formation rate is much smaller, only $\sim 1 M_{\odot} \text{ yr}^{-1}$, implying an star-formation efficiency of only

$$\epsilon_{\text{ff}} \lesssim 0.01$$

**star formation efficiency =
the mass fraction of a cloud that ultimately turns into stars in a unit time interval**

- The reasons for this are not entirely clear, but may stem in part from inhibition of gravitational collapse by **interstellar magnetic fields**, and/or by **interstellar turbulence**.
- Another likely factor is the **feedback from hot, massive stars**, which heat up and ionize the cloud out of which they form, thus preventing the further gravitational contraction of the cloud into more stars.

Fragmentation into Cold Cores

- Fragmentation

- In those portions of a GMC that do undergo gravitational collapse, the contraction soon leads to higher densities, and thus to smaller Jeans mass and Jeans radius, along with a shorter free-fall time.

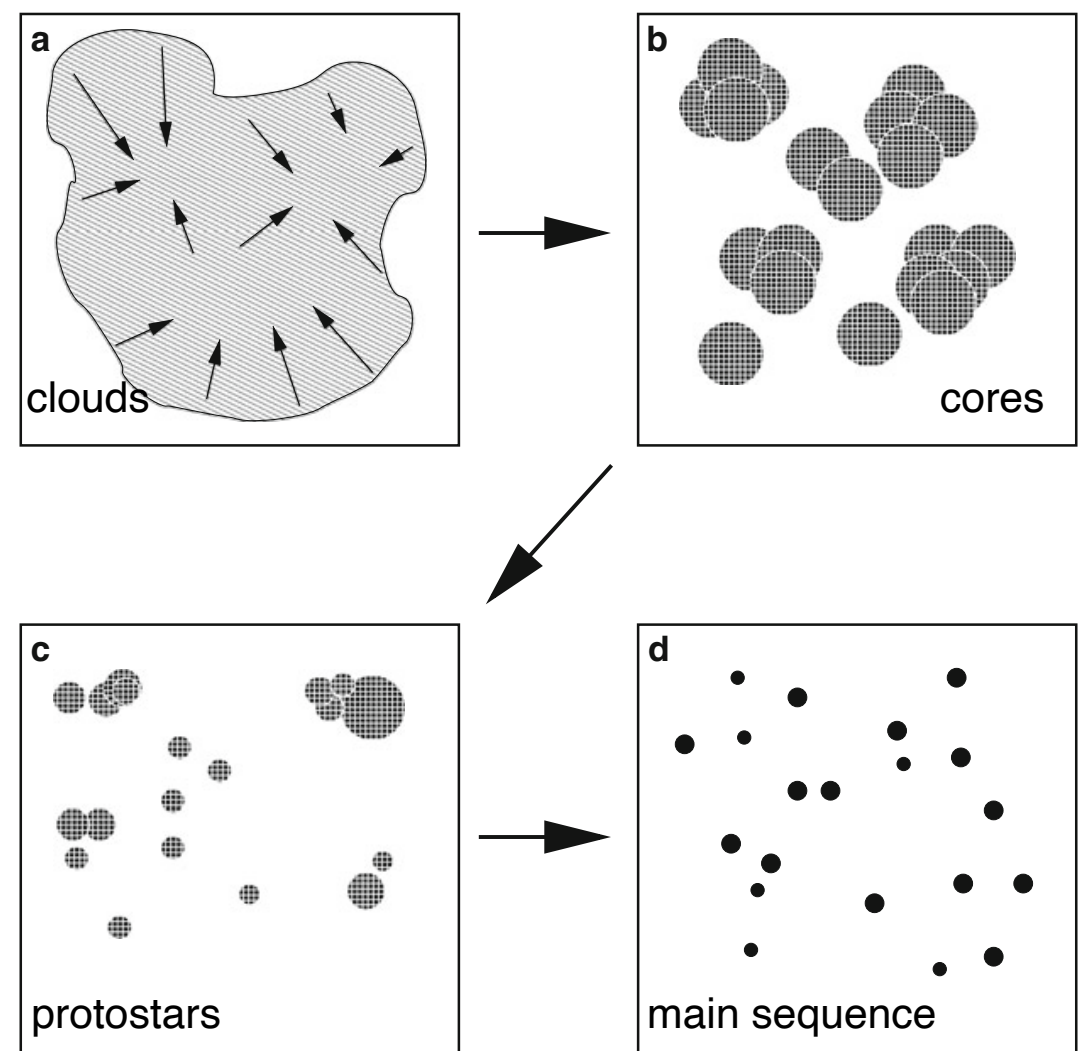
because $M_J \propto \rho^{-1/2}$, $R_J \propto \rho^{-1/2}$, and $t_{\text{ff}} \propto \rho^{-1/2}$

- This tends to cause the overall cloud, with total mass, to fragment into much smaller, stellar-mass cloud “cores” that will form into individual stars.

- The fragmentation process is a hierarchical process in which parent clouds break up into subclouds, which may themselves break into smaller structures.

- ◆ 10 kpc - spiral arms of the Galaxy
- ◆ 1 kpc - H I super clouds
- ◆ 100 pc - giant molecular clouds
- ◆ 10 pc - molecular clouds
- ◆ 0.1 pc - molecular cloud cores
- ◆ 100 AU - protostars

- Stars are the final step of fragmentation.



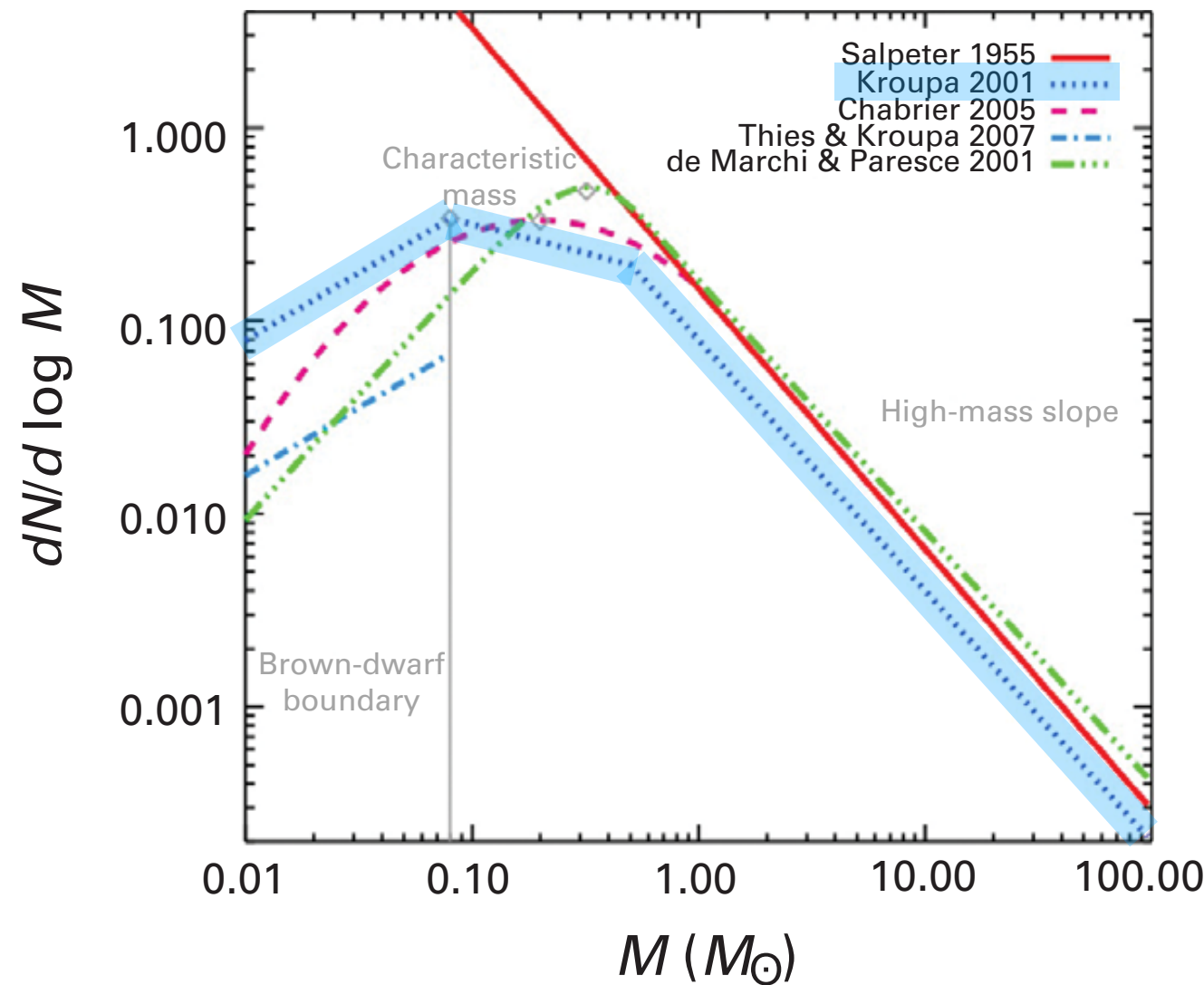
Initial Mass Function

- Initial Mass Function
 - A key, still-unsolved issue in star formation regards the physical processes and conditions that determine ***the mass distribution of these proto-stellar cores***, leading then to what is known as the stellar initial mass function (IMF).
 - ***IMF = the number of stars per a unit mass range as a function of mass.***
 - Studies of the evolution of stellar clusters suggest that this can be roughly characterized by a power-law form:

$$\frac{dN}{dm} = K m^{-\alpha} \quad (\alpha \approx 2.35 \text{ for } m > 1 M_{\odot}; \text{ Salpeter IMF})$$

- Here, K is a normalization factor that depends on the total number of stars. ***The large power-law index reflects the fact that higher-mass stars are much rarer than lower-mass stars.***

- More modern models generally flatten the distribution at lower-mass, as illustrated in the following figure. This allows them to be normalized to a finite number when integrated over all masses.



Comparison of IMFs from various authors.

Except for the Salpeter pure-power-law form, the curves are normalized such that the integral over mass is unity.

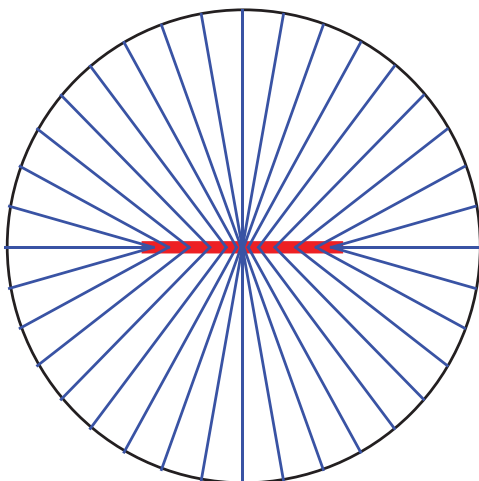
[Offner et al. 2014]

Kroupa IMF is the most commonly used one.

- With a given form of the IMF for a collapsing GMC, one can model the evolution of the resulting stellar cluster, based on how each star with a given mass evolves through its various evolutionary phases, e.g., main sequence, red giant, etc.

Formation of Planetary Disk - Angular Momentum Conservation

- Rotation is a ubiquitous phenomenon from the largest to the smallest scales in our Galaxy; the Galaxy itself rotates as a whole, its individual stars spin too.
- It is observed that molecular clouds do have a small amount of rotation, with velocities of order ***a few hundred meters per second*** ($\sim 0.15 \text{ km/s}$).
- In the same way as ice skaters spin faster as they pull in their arms, if all the angular momentum of the core were to be transferred to the star, it would rotate very rapidly.
- ***Stars cannot spin that fast because they would tear apart.*** Instead, the core may fragment as its density increases and form more than one star. The bulk of the core rotation then goes into orbital motion of multiple stars (and/or planets) rather than the rotation of a single star.



- ***The formation of “planets” around stars would not be possible if a certain amount of angular momentum was not present at the beginning of the star formation process.*** The angular momentum thus plays a significant role during the process of star and planet formation.

Core Collaps - Angular Momentum Transfer

- Eventually, this remnant disk-mass can fragment into its own gravitationally collapsing cores to form planets.
 - ◆ In our solar system, the most massive planet Jupiter has only 0.1% the mass of the Sun, but 99% of the solar system's angular momentum.
 - ◆ Earth too originated from the evolving proto-solar disk.

Young Stellar Objects (YSOs)

- Young Stellar Object denotes a star in its early stage of evolution.
 - ◆ This class consists of two groups of objects: protostars and pre-main-sequence stars.
 - ◆ A **protostar** is a very young star that is still gathering mass from its parent molecular cloud.
 - ▶ A dense core is initially in balance between self-gravity and gas/magnetic pressure. As the dense core acquires mass from its larger, surrounding cloud, self-gravity begins to overwhelm pressure, and collapse begins. **The protostellar phase begins when the molecular cloud fragment first collapses under the force of self-gravity and an opaque, pressure supported core forms inside the collapsing fragment.**
 - ▶ The gas that collapses toward the center of the dense core first builds up a low-mass protostar, and then a protoplanetary disk orbiting the object. As the collapse continues, an increasing amount of gas impacts the disk rather than the star, a consequence of angular momentum conservation.
 - ◆ The protostellar phase ends when the infalling gas is depleted, leaving a **pre-main-sequence star (PMS)**.
 - ▶ **After the protostar blows away the envelope, it is optically visible, and appears on the Hayashi track** in the Hertzsprung-Russell diagram. A pre-main-sequence star contracts to later become a main-sequence star at the onset of hydrogen fusion producing helium.
 - ▶ **The energy source of PMS objects is gravitational contraction**, as opposed to hydrogen burning in main-sequence stars.

• **Protostar**

- **Maximum infall rate:** Combining the free-fall timescale and maximum stable core mass, we can derive an upper limit to the mass infall rate.

$$\dot{M}_{\text{in}} = \frac{M_{\text{BE}}}{t_{\text{ff}}} \approx 2.2 \frac{c_s^3}{G}$$

$$\approx 4 \times 10^{-6} M_\odot/\text{yr}$$

←

$$M_{\text{BE}} = 1.5 \left(\frac{2}{\pi G^3 \rho} \right)^{1/2} c_s^3$$

$$t_{\text{ff}} = \left(\frac{3\pi}{32G\rho} \right)^{1/2}$$

- **Accretion luminosity:** This is high enough that the release of gravitational energy, as gas falls from core to stellar scales, provides significant accretion luminosity.

$$L_{\text{acc}} = -GM\dot{M}_{\text{in}} \left(\frac{1}{R_{\text{core}}} - \frac{1}{R_*} \right)$$

$$\approx 9.3 \left(\frac{M}{1 M_\odot} \right) \left(\frac{\dot{M}_{\text{in}}}{10^{-6} M_\odot \text{ yr}^{-1}} \right) \left(\frac{R_*}{3R_\odot} \right)^{-1} L_\odot$$

← core radius $R_{\text{core}} \gg$ stellar radius R_*
typical size of solar-mass stars at early
times $R_* \approx 3R_\odot$

- This calculation shows that **a protostar is detectable well before it begins nuclear fusion.**
- Due to the high dust extinction of the surrounding core, the very earliest phase of star formation is only visible at $\lambda > 100 \mu\text{m}$.

- But, within $\sim 10^5$ yr after collapse, protostars become detectable in the near-IR and mid-IR.
- As the core is used up, both the dust emission and extinction decrease. The protostar becomes increasingly visible at shorter wavelengths and the longer wavelength emission decreases.
- The evolutionary state of a protostar is generally classified based on its IR SED, but mm wavelength imaging of its surrounding envelope and disk is increasingly used in addition (e.g., ALMA).

- **Pre-main sequence star**

- Once the collapse phase ends and the protostar had reached its final mass, it is known as a pre-main sequence star.
- It slowly contracts through the loss of gravitational energy by radiation on a **Kelvin-Helmholtz timescale (thermal timescale)**, which determines how quickly a star contracts before nuclear fusion starts - i.e. sets roughly the pre-main sequence lifetime

$$t_{\text{KH}} = \frac{U}{L_*} = \frac{GM_*^2/R_*}{L_*} \simeq 31.1 \left(\frac{M_*}{M_\odot} \right)^2 \left(\frac{R_*}{R_\odot} \right)^{-1} \left(\frac{L_*}{L_\odot} \right)^{-1} \text{Myr}$$

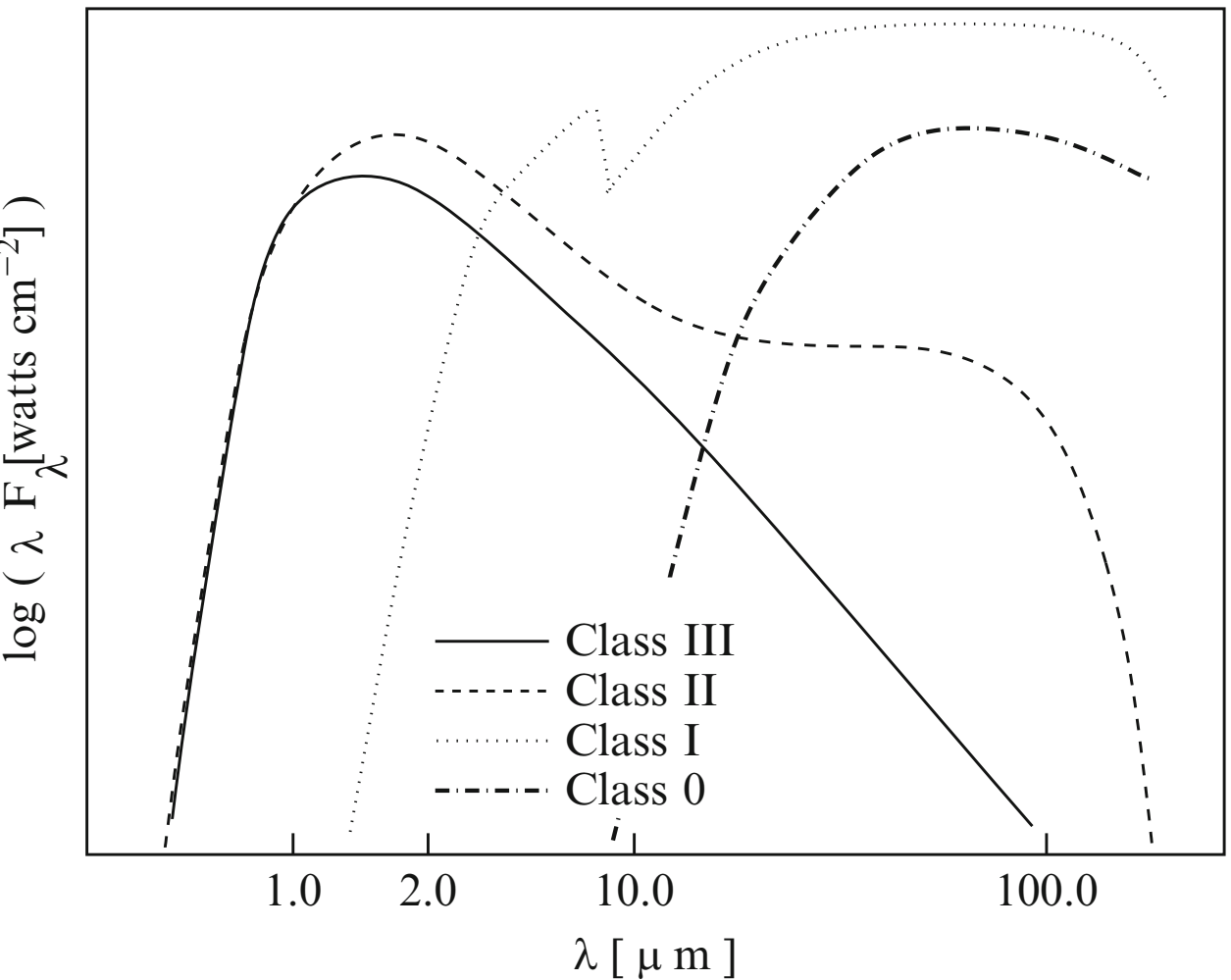
Kelvin-Helmholtz instability occurs when there is velocity shear.

Here, U = internal thermal energy (= gravitational potential) from the Virial theorem

- Pre-main sequence stars with $0.1 M_\odot < M_* < 2 M_\odot$ is known as **T Tauri stars**. These stars were first known in the 1940s and this name remains a common alternative name for pre-main sequence stars for historical reasons
- The intermediate mass counterpart, $2 M_\odot < M_* < 8 M_\odot$, are known as **Herbig Ae/Be stars**, where A and B refer to the stellar spectral types. The “e” denotes the photospheric emission lines that were used to identify their youth.
- **More massive stars are much more luminous and they contract too quickly. Hence, they have no pre-main-sequence stage.** By the time they become visible, the hydrogen in their centers is already fusing and they are main-sequence objects.

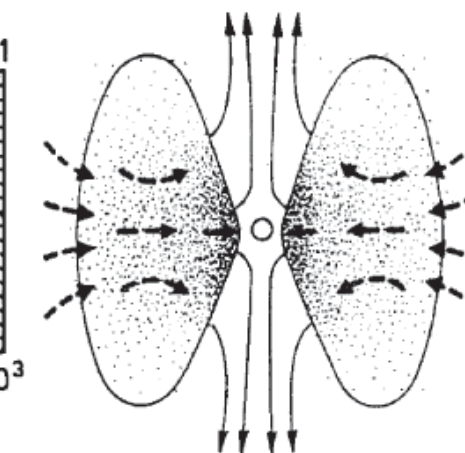
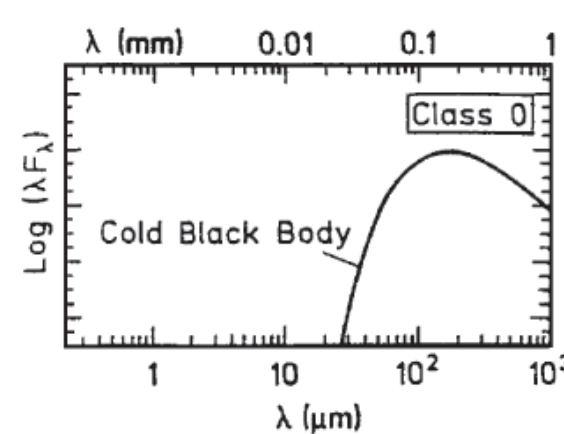
Spectral Energy Distributions (SEDs) of YSOs

- Lada & Wilking (1984) and Lada (1987) investigated SEDs of IR sources observed in the $1\text{-}100 \mu\text{m}$ wavelength band in the core of the Ophiuchi dark cloud, and proposed a general IR classification scheme.
 - ◆ A spectral index is defined between 2.2 and $25 \mu\text{m}$:
$$\alpha_{\text{IR}} = \frac{d \log(\lambda F_\lambda)}{d \log \lambda} \quad \lambda F_\lambda \propto \lambda^\alpha$$
 - ◆ Class I sources have very broad SEDs with $\alpha_{\text{IR}} > 0$.
 - ◆ Class 2 sources have $-2 < \alpha_{\text{IR}} < 0$.
 - ◆ Class 3 sources have $\alpha_{\text{IR}} < -2$.
 - ◆ The large IR excesses are attributed to thermal emission from dust in large circumstellar envelopes and Class I sources are likely to be evolved protostars.
- Andre et al. (1993) discovered embedded sources that remained undetected below $25 \mu\text{m}$ indicating significantly larger amounts of circumstellar material than in Class I sources and they proposed a younger Class 0 of YSOs.

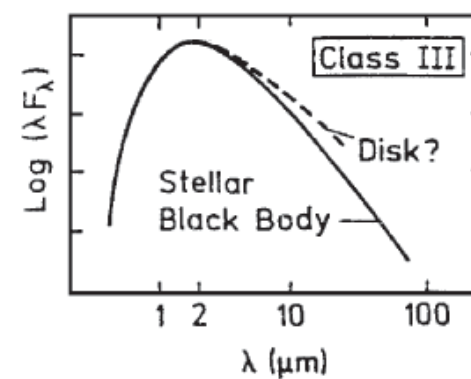
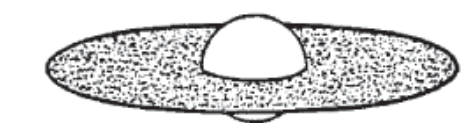
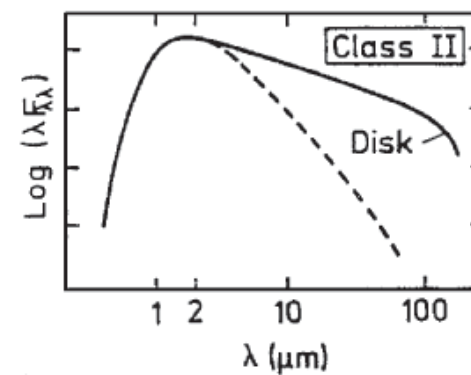
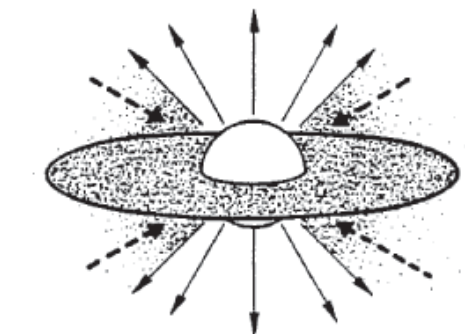
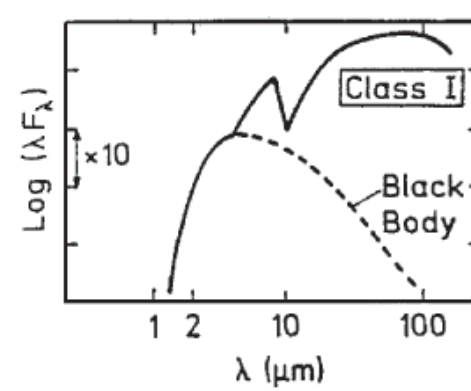


YSO classification

Protostars



Pre-Main Sequence Stars

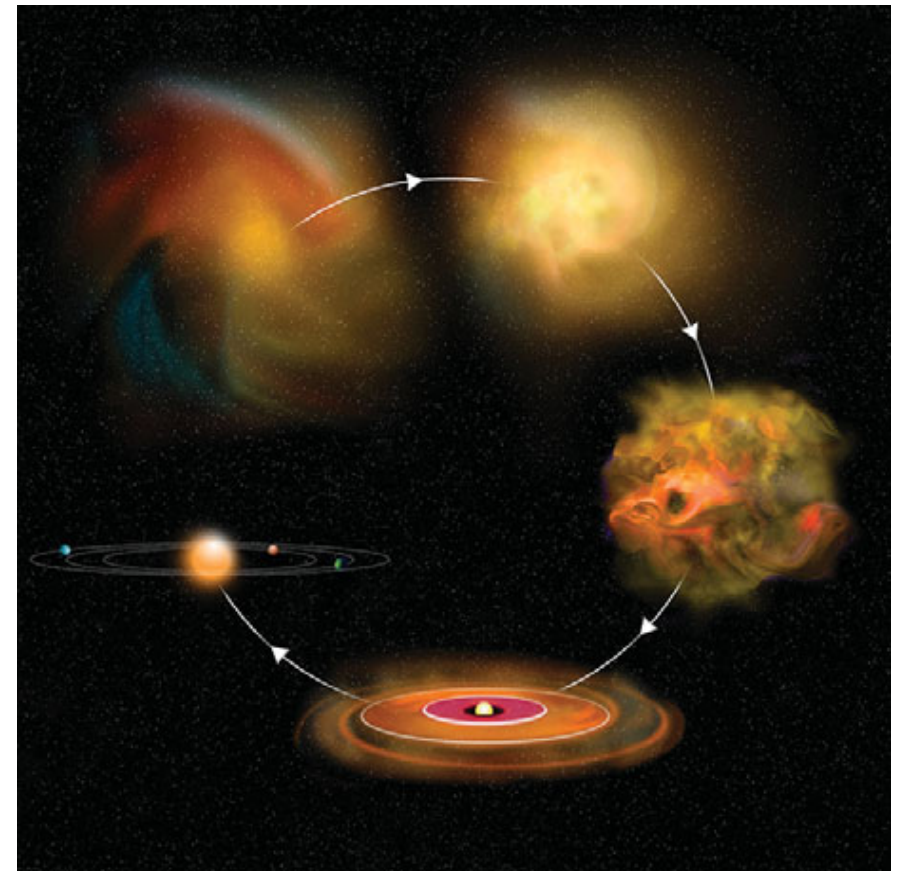


Andre (1994)

Planets

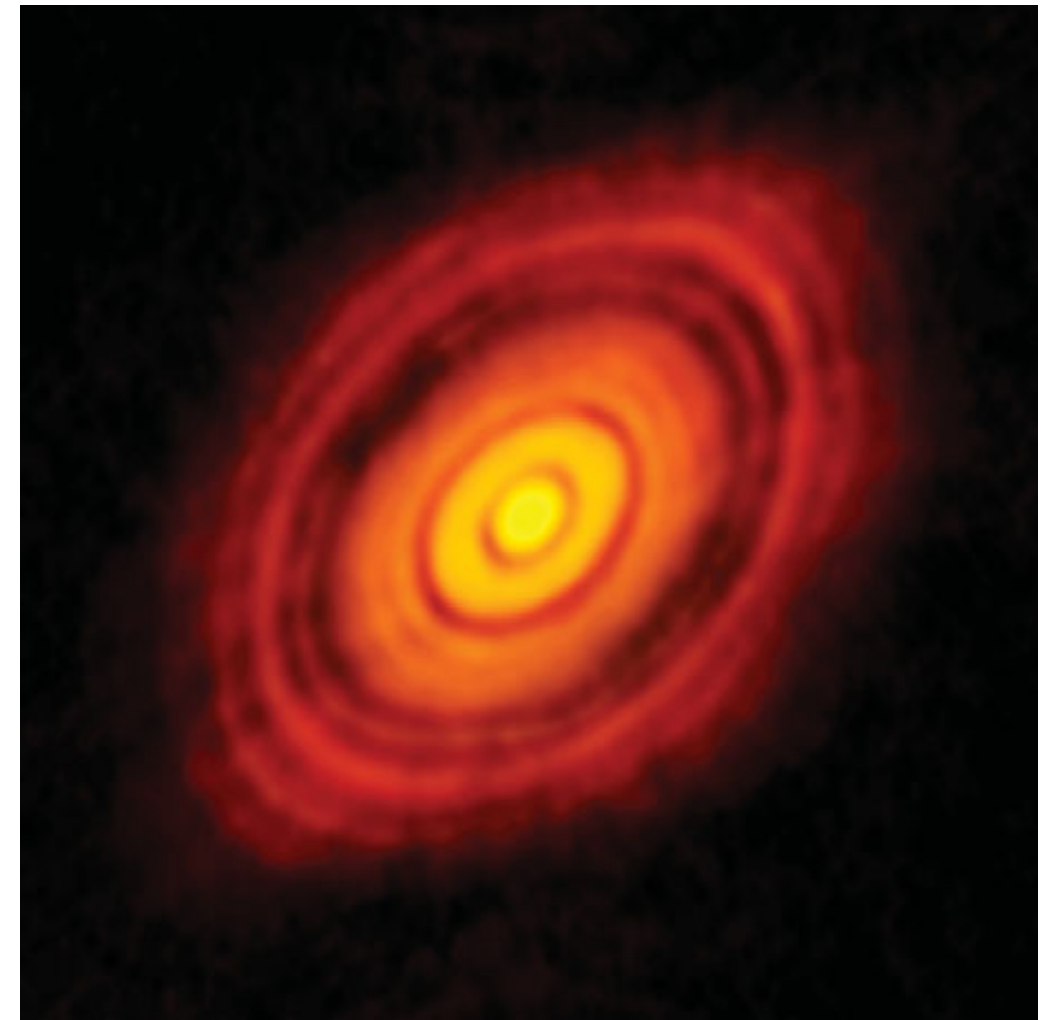
Origin of Planetary Systems

- The Nebular Model (basic ideas by Kant and Laplace)
 - The disk-formation process forms the basis for the “nebular model” for the formation of planetary systems, including our own solar system.
 - As a proto-stellar cloud collapses under the pull of its own gravity, conservation of its initial angular momentum leads naturally to form of an orbiting disk, which surrounds the central core mass.
 - This disk is initially gaseous, held **in a vertical hydrostatic equilibrium** about the disk mid-plane, **with radial support against gravity provided by the centrifugal force**.
 - This stops the rapid, dynamical infall, but as the viscous coupling between differentially rotating rings (and the entrainment of disk material by an outflowing stellar wind) transports angular momentum outward, there remains relatively slow inward diffuse flow of material that causes much of the initial disk mass to gradually accrete onto the young star.
 - This gradually depletes H and He gas (over a few million years). During this period, the heavier elements can gradually bond together to make molecules.
 - These in turn nucleate into grains of dust, and eventually into rocks.
 - Collisions among these rocks leads to a combination of fragmentation and accumulation, with the latter eventually forming asteroid-size (m to km) bodies. These then make planetoids, and eventually planets.



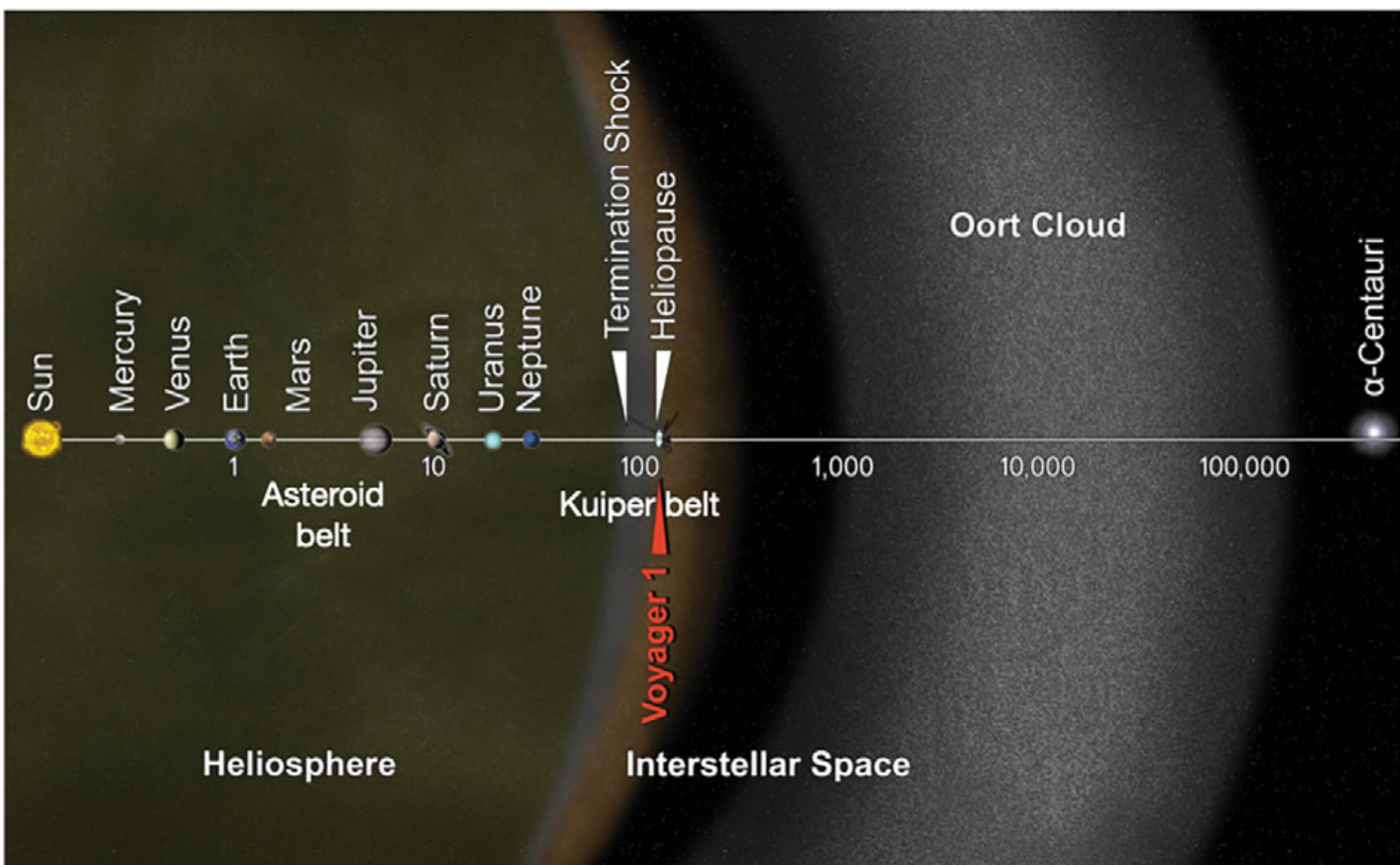
Observations of Proto-Planetary Disks

- Young stellar objects (YSOs) often show clear evidence of proto-planetary disks.
- With advent of telescope array (e.g., ALMA) observing in the far-IR and submm spectral regions, it is now becoming possible to image such disks directly.
- The figure shows an ALMA image of a proto-planetary disk in the T Tauri star HL Tauri, made in mm wavelengths.
- Interferometry from the array allows spatial resolution ranging down to **0.025 arcsec**. At HL Tauri's distance of 140 pc, this corresponds to **3.5 AU**, with the visible disk extending over a diameter of ~ 200 AU.
- ***The disk gaps likely represent regions where planet formation is clearing out disk debris,*** though there is so far no direct evidence of fully formed planets in this system.
- A key issue in planet formation is whether this can occur quickly enough to compete with disk depletion by various processes, like accretion onto the star, dissociation by stellar UV radiation, and entrainment in a outflowing stellar wind.



Our Solar System

- Planets
 - Rocky planets (rocky dwarfs; terrestrial planets): Mercury, Venus, Earth, Mars
 - Gas giants: Jupiter and Saturn
 - Ice giants: Uranus and Neptune



- **Snow line** (also known as the **ice line** or **frost line**)

- the particular distance in the solar nebula from the central protostar where it is cold enough for volatile compounds such as water, ammonia, methane, carbon dioxide, and carbon monoxide to condense into solid ice grains. The frost line separates terrestrial planets from giant planets in the Solar system.

In the solar system, the distance for the snow line is ~ 3 AU, between Mars and Jupiter

- In the colder outer regions, these condensed to form ice, which gradually collected into ever larger solid cores, eventually growing massive enough to gravitationally attract and retain the even more abundant but lighter gases of hydrogen and helium.
 - ◆ This is the basis for formation of the outer gas and ice giant planets, with an overall composition similar to the solar nebula, and the present day Sun.
- In the inner nebula, where it was too warm to form ice, such light atoms of H and He escaped from the weaker gravity of the smaller, rocky planets, effectively preventing their growth and so keeping them relatively small.

- **Hot Jupiter**

- a planet with a mass comparable to (actually even larger than) Jupiter, but orbiting at such a close distance that the stellar heating would make it quite hot.
- Such gas giants had been supposed to form only beyond the ice line. The detection of hot Jupiters around several stars was a real surprise.
- They are thought to have formed outside the snow line, and later migrated inwards to their current positions. Gravitational interaction with the proto-stellar disk and/or other giant planets out there is supposed to lead some to be flung into an inward migration, so that they finally ended up very close to their star.

Detection of Exoplanets (Extra-solar planets)

- Direct-Imaging Method

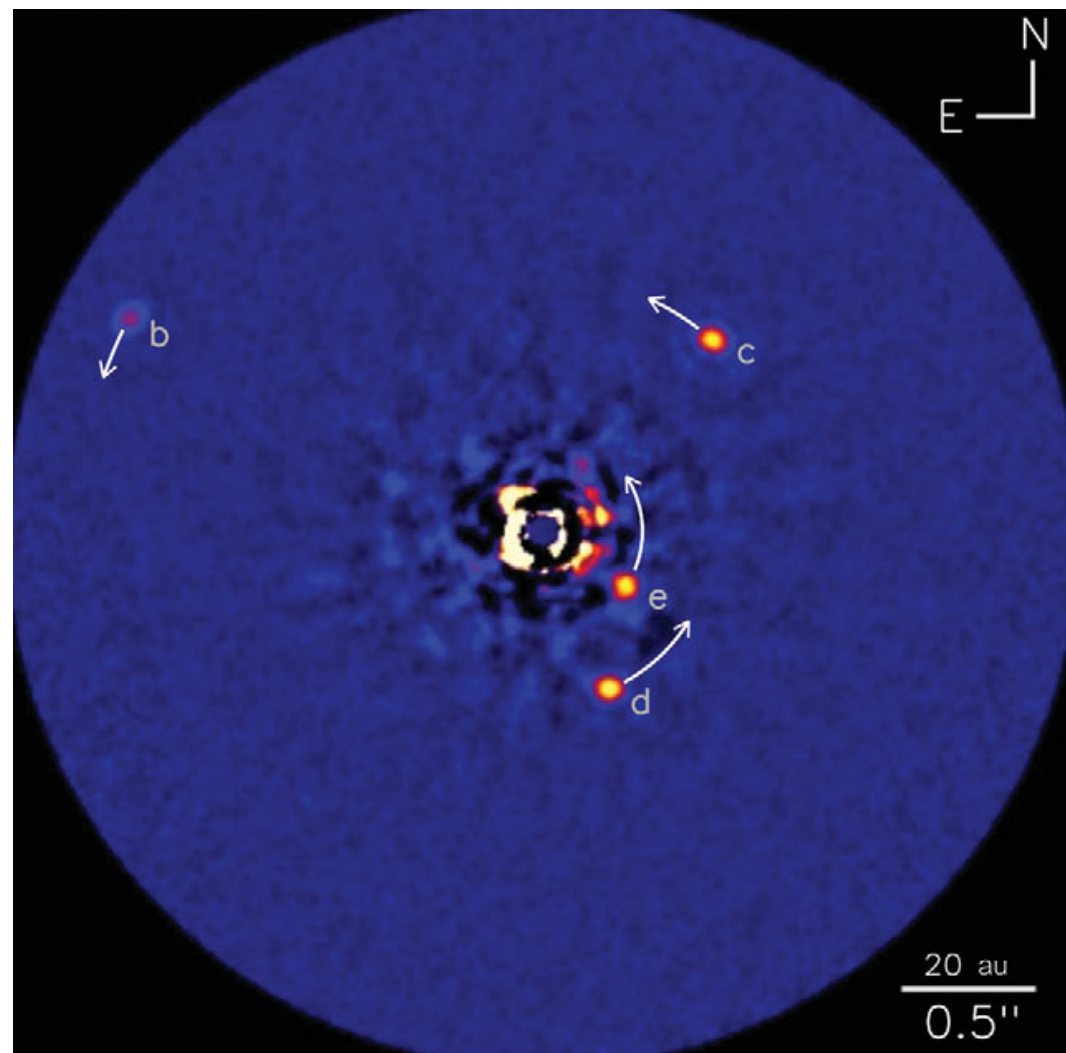
- Because they are much cooler than stars, the thermal emission from planets is mostly in the IR.
- Their appearance at visible wavelengths comes by reflected light from their host stars. This greatly complicates direct detection of extra-solar planets, since this reflected light is generally overwhelmed by the direct light from the stars.
- Nowadays, there are ~ 20 such detect imaging detections of exoplanets.

Direct image by the Keck Observatory of 4 exoplanets orbiting HR8799.

The arrows indicates their orbital motion from monitoring their positions over more than a decade. The orbital periods are 49, 100, 189, and 474 years for planets e, d, c, and b, respectively.

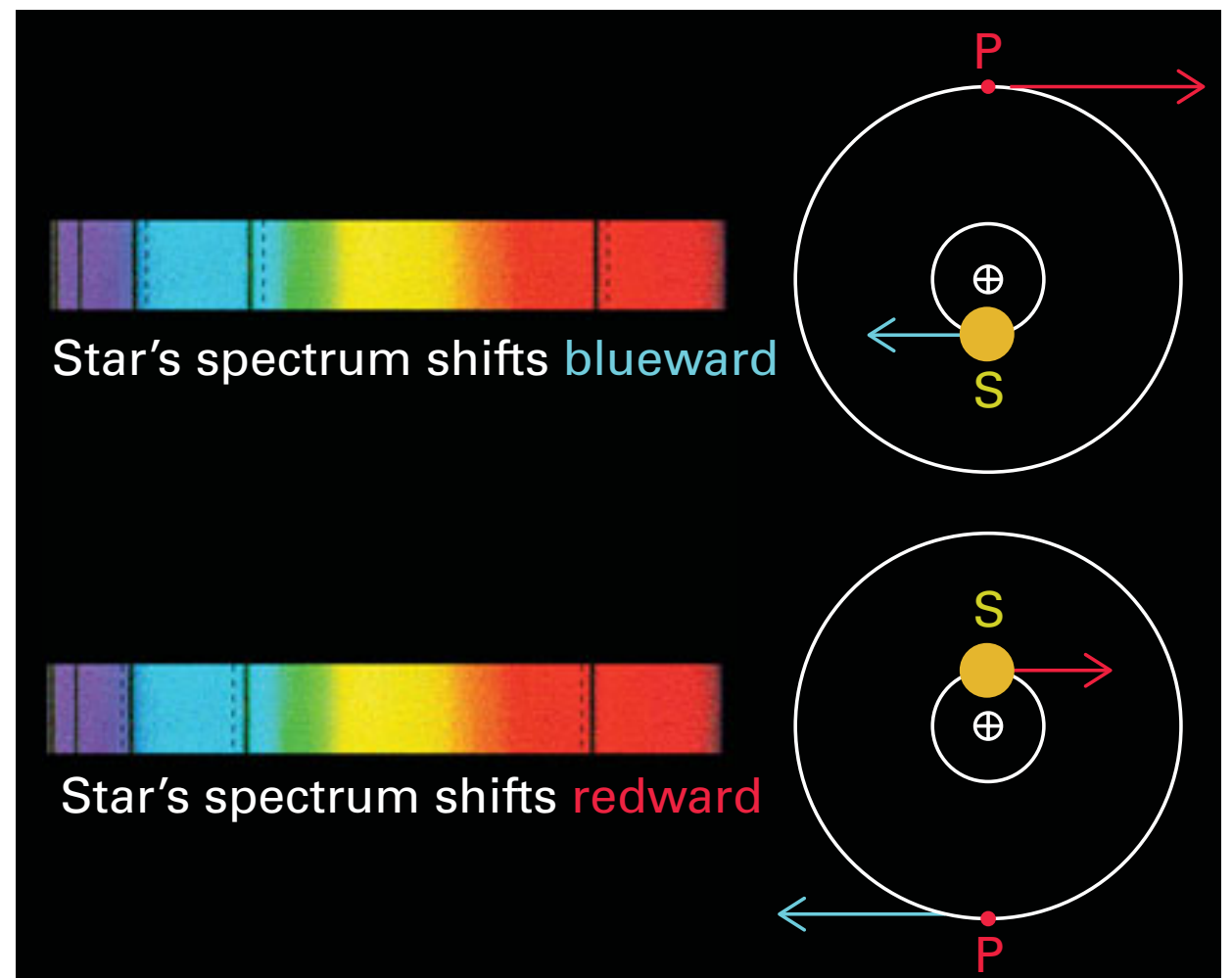
For reference, the orbital period of Neptune is 165 years.

[NTV-HIS/C. Marois/W. M. Keck Observatory]



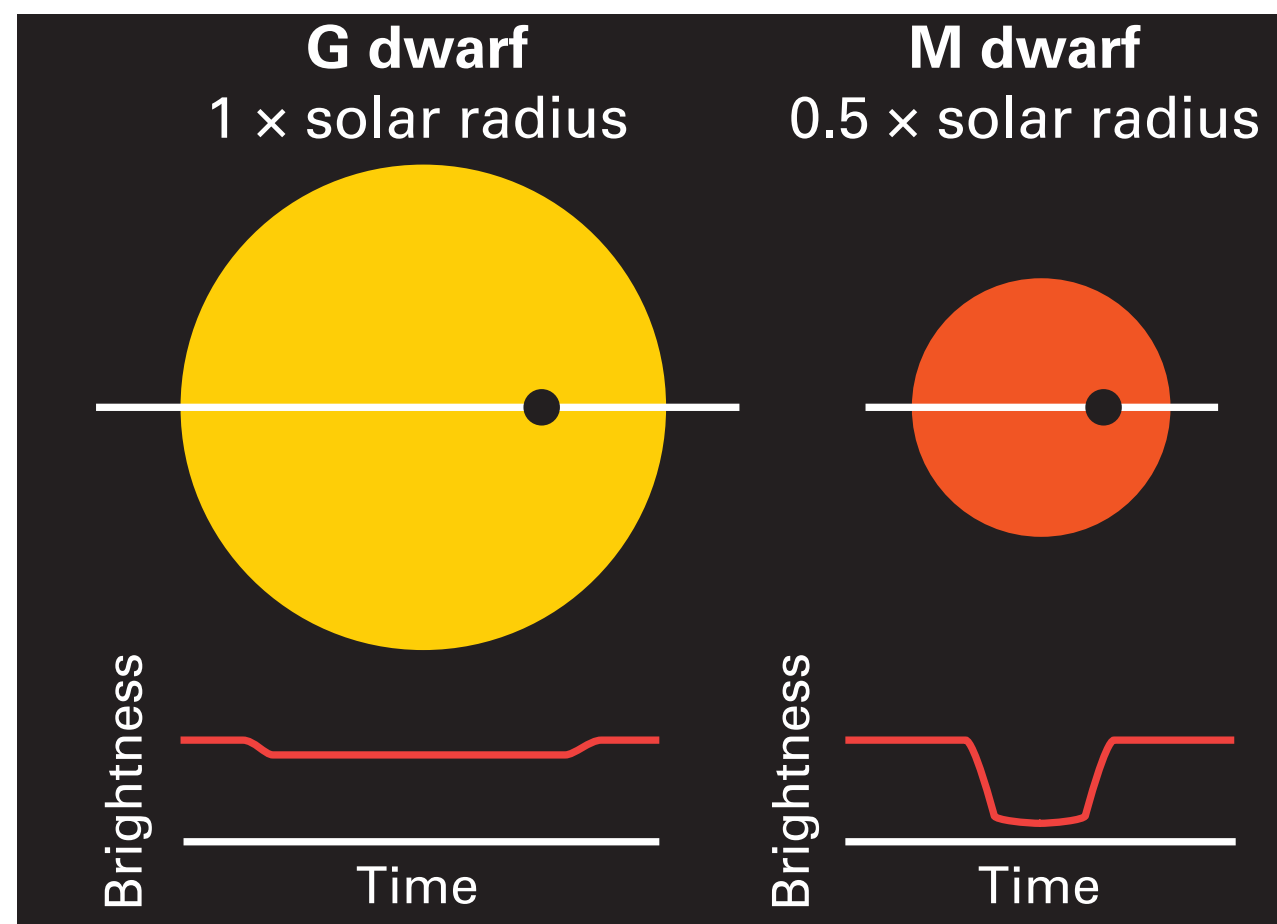
- Radial-Velocity Method

- The periodic movement of the host star due to the gravitational pull of the planet causes spatial “**wobble**.”
- This wobble is not directly detectable, but, its associated motion toward and away from the observer can be detected via **very precise spectroscopic measurements** of the systematic Doppler shift from multiple absorption lines in the star’s spectrum.
- This is the same method as used in spectroscopic binaries.



-
- Transit Method
 - This method simply looks for the slight dimming of the star's apparent brightness whenever a planet “transits” in front of it.
 - Instead of elaborate spectroscopic measurement of the slight Doppler shift, this merely requires **precise photometric measurements** of changes in the star's total apparent brightness. (This is analogous to eclipsing binaries)
 - The fractional drop in the star's brightness will be

$$\frac{\Delta F}{F} = \left(\frac{R_p}{R_*} \right)^2$$

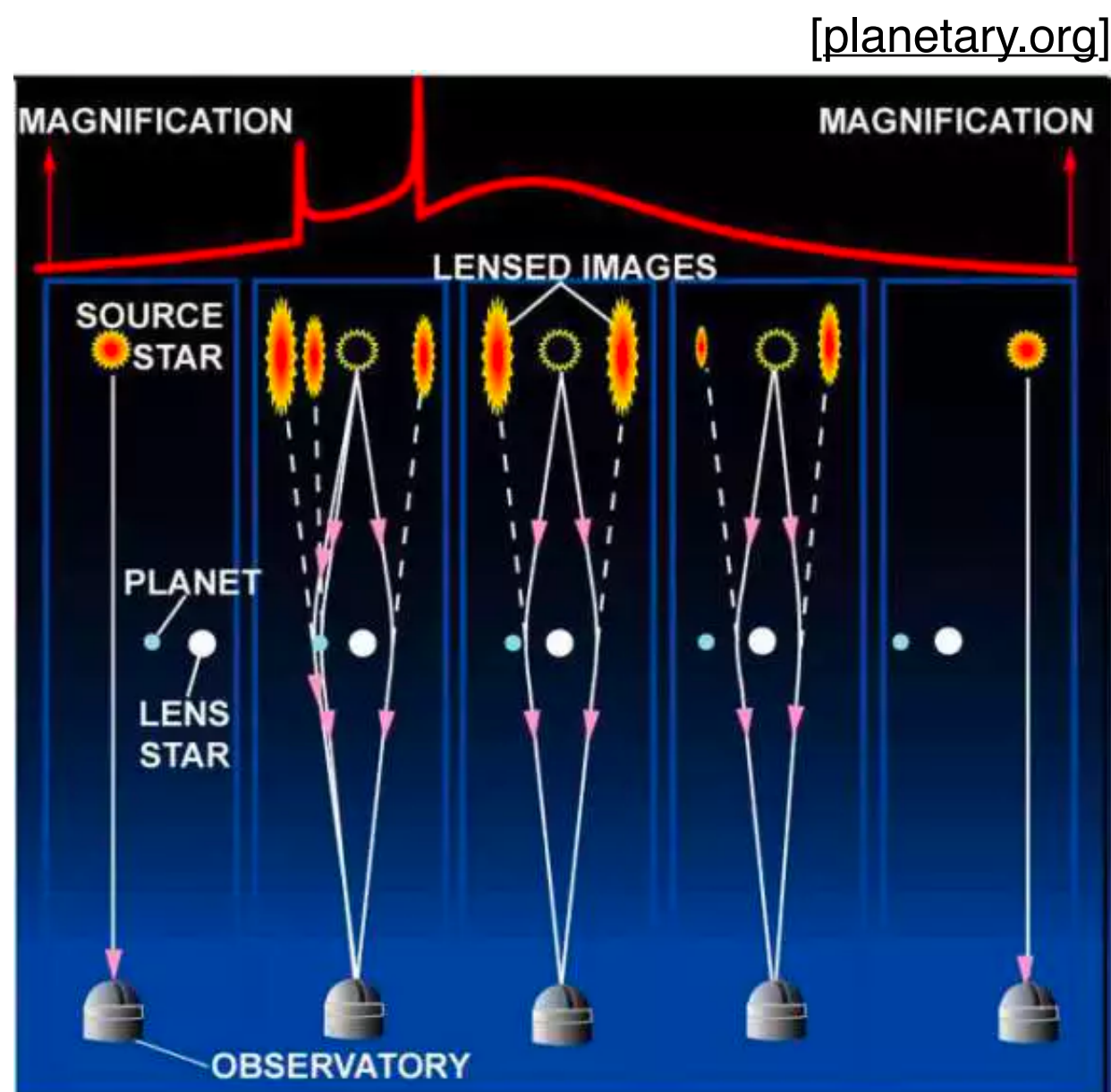


- Microlensing Method

- Microlensing is a form of gravitational lensing in which the light from a background source is bent by the gravitational field of a foreground lens to create distorted, multiple and/or brightened images.

The lensing star (white) moves in front of the source star (yellow) magnifying its image and creating a microlensing event.

In the second image (from left), the planet adds its own microlensing effect, creating the two characteristic spikes in the light curve.



Homework (due date: 04/07) - to be updated

[Q5]

If the dust extinction A_λ were a power law in the wavelength, $A_\lambda \propto \lambda^{-\alpha}$, what would be R_V as a function of α ?

What value of α would give $R_V = 3.1$?

[Q6] - Virial Theorem

Read the section 2 of the following reference:

<https://www.uio.no/studier/emner/matnat/astro/nedlagte-emner/AST1100/h09/undervisningsmateriale/lecture5.pdf>

The above reference derives the potential energy for a spherical cloud with a uniform density.

(You may want to read the section 1 for the proof of the Virial theorem.)

Consider a spherical cloud with a total mass M and a radius R . Assume that the cloud has a radial density profile of $\rho = \rho_0(r/R)^{-\beta}$ (Eq-1). It can easily proved that the gravitational potential energy can be expressed as Eq-2:

$$[\text{Eq-1}] \rho = \rho_0 \left(\frac{r}{R} \right)^{-\beta} \rightarrow [\text{Eq-2}] U = -\alpha \frac{GM^2}{R}$$

- (a) Refer to the above reference and derive the formula for gravitational potential energy (Eq-2) in the case of the density profile given by Eq-1. For Eq-2 to be satisfied, what is (are) the condition(s) for β ?
- (b) Express α in terms of β .